
PlatoLTL: Learning to Generalize Across Symbols in LTL Instructions for Multi-Task RL

Jacques Cloete¹ Mathias Jackermeier² Ioannis Havoutis¹ Alessandro Abate²

Abstract

A central challenge in multi-task reinforcement learning (RL) is to train generalist policies capable of performing tasks not seen during training. To facilitate such generalization, linear temporal logic (LTL) has recently emerged as a powerful formalism for specifying structured, temporally extended tasks to RL agents. While existing approaches to LTL-guided multi-task RL demonstrate successful generalization across LTL specifications, they are unable to generalize to unseen vocabularies of propositions (or “symbols”), which describe high-level events in LTL. We present PlatoLTL, a novel approach that enables policies to zero-shot generalize not only *compositionally* across LTL formula structures, but also *parametrically* across propositions. We achieve this by treating propositions as instances of parameterized predicates rather than discrete symbols, allowing policies to learn shared structure across related propositions. We propose a novel architecture that embeds and composes predicates to represent LTL specifications, and demonstrate successful zero-shot generalization to novel propositions and tasks across challenging environments.

1. Introduction

A key challenge in robotics and artificial intelligence (AI) is to create agents capable of performing arbitrary complex, long-horizon tasks. A rapidly-growing *neuro-symbolic* paradigm uses formal languages to define task objectives and guide the learning of policies in frameworks such as reinforcement learning (RL). Accordingly, Linear Temporal Logic (LTL; Pnueli, 1977) has recently been adopted as a powerful formalism for specifying complex, temporally-extended and non-Markovian tasks in RL (Hasanbeig et al.,

¹Oxford Robotics Institute, University of Oxford, Oxford, United Kingdom ²Department of Computer Science, University of Oxford, Oxford, United Kingdom. Correspondence to: Jacques Cloete <jacques@robots.ox.ac.uk>.

2023). Recent approaches such as DeepLTL (Jackermeier & Abate, 2025) learn policies that can zero-shot generalize across LTL specifications.

However, the applicability of these methods to real-life domains such as robotics remains limited, due to the necessity of composing all valid LTL specifications from a fixed, discrete vocabulary of *atomic propositions* known a priori. Instead, many tasks in domains such as robotic manipulation are parameterized by one or more continuous variables; for example, a robot may need to pick up a particular object obj , place an object at a particular position (x, y) on a table, twist a valve by a particular angle θ , or press a button with a particular force F . These parameters may be different between task instances, or even within the same instance (e.g., placing two objects in two different locations). To generalize to arbitrary task instances, existing LTL-guided RL approaches would require an infinite number of different propositions defined a priori, which can be impractical.

To overcome this, we propose reformulating atomic propositions as instances of *atomic predicates* with particular parameter values; the predicates are non-quantified variables that represent truth statements about an environment in relation to the given parameters. By conditioning the policy on LTL formulae described in terms of these predicates, the policy learns to generalize not only across LTL task structures, but also across predicate parameters. Since new propositions are now just new instances of the same atomic predicates with different parameters, our approach can even generalize to propositions unseen during training. This greatly enhances the scalability of LTL-based RL to real-world scenarios. By an appropriate choice of predicate parameterization, the policy can learn useful, grounded associations between task parameters and the environment so as to improve both training and generalization.

We implement our approach as PlatoLTL (Parameterized logic architecture for temporal objectives in LTL), which learns generalist policies for arbitrary LTL specifications with parameterized atomic propositions.

The main contributions of this work are as follows:

1. We propose that, for many problems, the atomic propositions used to compose a LTL specification can be

reformulated as instances of *atomic predicates* with particular parameter values.

2. We present a novel neural network architecture that meaningfully maps predicate parameters to proposition embeddings, and uses these embeddings to construct embeddings of *reach-avoid sequences* of Boolean formulae representing the LTL specification.
3. Hence, we present PlatoLTL, a novel LTL-guided RL approach that zero-shot generalizes both *compositionally* across different LTL formula structures, and *parameterically* across atomic propositions.
4. We introduce two novel benchmark environments, *RG-BZoneEnv* and *FalloutWorld*, which extend two existing benchmarks to admit complex LTL specifications composed from a large (or even infinite) vocabulary of atomic propositions.
5. We empirically validate¹ the effectiveness of PlatoLTL on a range of tasks in the aforementioned environments, demonstrating its ability to generalize to atomic propositions unseen during training.

2. Related Work

Methods for learning LTL-guided policies can generally be classified into two broad approaches. The “hierarchical” approach first converts the LTL formula into an automaton, which is treated as a kind of reward machine (Icarte et al., 2018; 2022; Camacho et al., 2019). The agent learns a sub-policy for each automaton state or transition, creating a hierarchy wherein the automaton acts as the high-level policy and the sub-policies are the options (Yuan et al., 2019; Hahn et al., 2019; Jothimurugan et al., 2019; 2021; Bozkurt et al., 2020; Hasanbeig et al., 2020; 2023; Cai et al., 2021; Voloshin et al., 2023; Shukla et al., 2024; Shah et al., 2025). However, such methods are generally capable of producing only *single-task* policies, since the states of the automaton correspond only to a particular LTL specification. In comparison, our work takes the “goal-conditioned” approach, conditioning the policy on a learned representation of the LTL formula (León et al., 2022; Qiu et al., 2023; Yalcinkaya et al., 2024; Xu & Fekri, 2024; Giuri et al., 2025); by training a policy over a distribution of such representations, one can obtain *multi-task* policies.

LTL2Action (Vaezipoor et al., 2021) encodes the syntax tree of the task LTL specification using a Graph Neural Network (GNN; Zhou et al., 2020), updating the specification via LTL progression as the agent progresses through the task. Meanwhile, DeepLTL (Jackermeier & Abate, 2025) extracts a reach-avoid sequence of sets of assignments for LTL satisfaction from its corresponding automaton, and uses a Recurrent Neural Network (RNN; Sherstinsky, 2020)

to embed the sequence, updating it as the agent satisfies each subgoal. DeepLTL in particular enables very efficient curriculum learning of long-horizon tasks. Recently, Transformers have been used to generate task embeddings from LTL formulae (Zhang et al., 2023; 2024), though it has been shown that, in model-free RL settings, Transformers often struggle to learn the complex interactions needed for LTL specifications (Giuri et al., 2025). However, the applicability of these methods to real-life domains such as robotics remains limited by composing all valid LTL specifications from a *fixed and discrete* vocabulary of atomic propositions known a-priori, each requiring their own labeling function from environment observations to proposition truth values. The generalizability of the policy is thus constrained by the expressiveness of the vocabulary it was trained on; if a new LTL specification uses a proposition unseen during training, the policy is not able to generalize to that specification (Vaezipoor et al., 2021; Jackermeier & Abate, 2025). In comparison, our work enables *parametric* generalization by treating propositions as instances of atomic predicates with particular parameter values.

Other work has experimented with parameterizing LTL specifications, but these methods either learn single-task policies (Jothimurugan et al., 2019; 2021; Shukla et al., 2024), or the simple parameter embedding scheme they use severely restricts the space of tasks, often to sequential reach tasks of one proposition each (Hatanaka et al., 2025). In comparison, our work remains expressive enough to admit *arbitrary* LTL formulae by using parameterization to obtain meaningful embeddings of the atomic propositions, from which an embedding of the task is then composed. Promising work by Guo et al. (2025) demonstrates efficient generalization to unseen propositions by remapping portions of the observation space into universal “reach” and “avoid” observations, but relies on the assumption that the observation space can be partitioned into proposition-specific observations, produced by identical observation functions under output transformation, which is not true (or may require significant environment-specific engineering) for general environments; our work makes no such assumptions, but instead assumes that the task propositions can be meaningfully reformulated as instances of atomic predicates.

3. Background

3.1. Reinforcement Learning

We consider a model-free reinforcement learning (RL) setup where an agent interacts with an unknown environment modeled as a *Markov Decision Process* (MDP; Sutton & Barto, 2014). An MDP is defined as a tuple $\mathcal{M} = \langle \mathcal{S}, \mathcal{A}, p, \mu, r, \gamma \rangle$, with state space \mathcal{S} and action space \mathcal{A} , where $p(s' | s, a) : \mathcal{S} \times \mathcal{A} \rightarrow \Delta(\mathcal{S})$ and $\mu(s) \in \Delta(\mathcal{S})$ are the (unknown) state-transition and initial state distributions,

¹All code will be publicly released upon publication.

respectively, $r(s, a, s') : \mathcal{S} \times \mathcal{A} \times \mathcal{S} \rightarrow \mathbb{R}$ is the reward function, and $\gamma \in [0, 1]$ is the discount factor. We aim to find a stochastic policy $\pi(a | s) : \mathcal{S} \rightarrow \Delta(\mathcal{A})$ that maximizes the *expected discounted return* $J(\pi) = \mathbb{E}_{\tau \sim \pi} [\sum_{t=0}^{\infty} \gamma^t r_t]$, where $\tau = (s_0, a_0, r_0, s_1, \dots)$ is a trajectory generated under policy π and state transition distribution p starting from $s_0 \sim \mu$, such that $a_t \sim \pi(\cdot | s_t)$, $s_{t+1} \sim p(\cdot | s_t, a_t)$, and $r_t = r(s_t, a_t, s_{t+1})$. The *value function* of a policy, $V^\pi(s) = \mathbb{E}_{\tau \sim \pi} [\sum_{t=0}^{\infty} \gamma^t r_t | s_0 = s]$, is the expected discounted return under policy π starting from state s .

3.2. Linear Temporal Logic

Linear temporal logic (LTL; Pnueli, 1977) is a formal logic that provides a human-readable formalism to specify properties (or specifications) over infinite trajectories. LTL is capable of expressing complex temporally-extended behaviors such as safety, liveness, recurrence and persistence (Manna & Pnueli, 1990). LTL formulae are composed from a finite set of *atomic propositions*, AP , which represent Boolean statements about the environment. The syntax of LTL is recursively defined as

$$\varphi ::= \top \mid p \mid \neg \varphi \mid \varphi \wedge \psi \mid X \varphi \mid \varphi \mathbf{U} \psi$$

where \top denotes true, $p \in AP$ is an atomic proposition, \neg (negation) and \wedge (conjunction) are standard Boolean operators, φ and ψ are LTL formulae, and X (next) and \mathbf{U} (until) are temporal operators. We define temporal operators F (eventually) and G (always) as $F\varphi \equiv \top \mathbf{U} \varphi$ and $G\varphi \equiv \neg F \neg \varphi$, respectively.

Let $\Sigma \subseteq 2^{AP}$ be the *alphabet*, in other words, the set of all permitted combinations of proposition truth values. Let $\sigma \in \Sigma$ be an *assignment*, i.e., the set of atomic propositions that are true at a given time. An ω -word $w = (s_0, \sigma_1, \sigma_2, \dots)$ is an infinite sequence of assignments; we denote the set of all ω -words over Σ as Σ^ω , such that $w \in \Sigma^\omega$. The satisfaction semantics of LTL are defined via the recursive satisfaction relation $w \models \varphi$. (See Appendix A for further details.)

To ground LTL specifications in an MDP, we assume access to a *labeling function* $L : \mathcal{S} \rightarrow \Sigma$, which returns the set of atomic propositions that are true, i.e., the assignment σ , for a given state s . A trajectory τ is mapped to a sequence of assignments via its trace $\text{tr}(\tau) = (L(s_0), L(s_1), \dots)$, and $\tau \models \varphi$ denotes shorthand for $\text{tr}(\tau) \models \varphi$. We thus define the *satisfaction probability* of an LTL formula φ under policy π in MDP \mathcal{M} as $P(\pi \models \varphi) = \mathbb{E}_{\tau \sim \pi} [\mathbb{1}[\tau \models \varphi]]$.

3.3. Büchi Automata

A more convenient way of reasoning about LTL satisfaction is to use *Büchi automata* (Büchi, 1966), which are finite-state machines that can be employed to express any LTL formula. Such automata can be used to monitor the progress towards satisfying a particular specification. In

the context of MDPs and particularly in this work, we use *limit-deterministic Büchi automata* (LDBAs; Sickert et al., 2016), which limit non-determinism to special transitions, called ϵ -transitions, and as such are particularly suitable for use alongside MDPs. An LDBA is defined as a tuple $\mathcal{B} = \langle \mathcal{Q}, q_0, \Sigma, \delta, \mathcal{F}, \mathcal{E} \rangle$, where \mathcal{Q} is the finite set of states, $q_0 \in \mathcal{Q}$ is the initial state, $\Sigma \subseteq 2^{AP}$ is the finite alphabet, $\delta(q, \sigma) : \mathcal{Q} \times (\Sigma \cup \mathcal{E}) \rightarrow \mathcal{Q}$ is the transition function, \mathcal{F} is the set of accepting states, and \mathcal{E} is the set of ϵ -transitions. Furthermore, \mathcal{Q} is partitioned into two subsets \mathcal{Q}_N (initial component) and \mathcal{Q}_D (accepting component), i.e., $\mathcal{Q} = \mathcal{Q}_N \uplus \mathcal{Q}_D$, such that $q_0 \in \mathcal{Q}_N$ and $\mathcal{F} \subseteq \mathcal{Q}_D$. Subsets \mathcal{Q}_N and \mathcal{Q}_D are closed and deterministic under non- ϵ -transitions, i.e., $\delta(q, \sigma) \in \mathcal{Q}_D$ for all $q \in \mathcal{Q}_D$ and $\sigma \in \Sigma$, and $\delta(q, \sigma) \in \mathcal{Q}_N$ for all $q \in \mathcal{Q}_N$ and $\sigma \in \Sigma$. To transition from \mathcal{Q}_N to \mathcal{Q}_D requires taking a non-deterministic ϵ -transition $\epsilon \in \mathcal{E}$. Taking an ϵ -transition does not consume an assignment, and thus ϵ -transitions can be thought of intuitively as *unobserved* jumps between two states.

Given an input ω -word w , a *run* $r = (q_0, q_1, q_2, \dots)$ of \mathcal{B} is an infinite sequence of states $q \in \mathcal{Q}$ respecting the transition function δ . An ω -word w is *accepted* by \mathcal{B} if there exists a run that infinitely often visits accepting states $q \in \mathcal{F}$. While LDBAs are *almost* deterministic, they retain the expressiveness of non-deterministic Büchi automata, and they can thus be used to represent any LTL specification. Given an LTL formula φ , it is possible to automatically construct an LDBA $\mathcal{B}_\varphi = \langle \mathcal{Q}_\varphi, q_0^\varphi, \Sigma_\varphi, \delta_\varphi, \mathcal{F}_\varphi, \mathcal{E}_\varphi \rangle$ such that \mathcal{B}_φ accepts exactly the ω -words w for which $w \models \varphi$ (Sickert et al., 2016). See Appendix B for an example.

4. Problem Setting

We use goal-conditioned RL (Liu et al., 2022) to learn a specification-conditioned policy $\pi(a | s, \varphi)$ that maximizes the probability of satisfying an LTL formula $\varphi \sim \xi$, where ξ is an arbitrary distribution over LTL formulae with support $\text{supp}(\xi)$. The optimal policy π^* in \mathcal{M} is thus defined as

$$\pi^* = \arg \max_{\pi} \mathbb{E}_{\substack{\varphi \sim \xi, \\ \tau \sim \pi | \varphi}} [\mathbb{1}[\tau \models \varphi]]. \quad (1)$$

To find solutions to Equation 1 via RL, we construct a *product MDP* \mathcal{M}^φ , which extends the state space of \mathcal{M} to monitor the state of LDBA \mathcal{B}_φ . Since the LDBA state encodes the memory necessary to satisfy φ , this allows policies conditioned on both MDP state and LDBA state to be memoryless (Baier & Katoen, 2008). Note that in practice we never explicitly construct the product MDP, but instead update LDBA state q^φ using the assignment $\sigma^\varphi = L_\varphi(s)$ observed at each time step.

We then obtain an approximate solution for Equation 1 by solving the following problem:

Problem 4.1 (Efficient LTL satisfaction; Jackermeier &

Abate, 2025). Given an unknown MDP \mathcal{M} , distribution over LTL formulae ξ , and LDBAs \mathcal{B}_φ for each $\varphi \in \text{supp}(\xi)$, find the optimal policy

$$\pi_{\text{eff}}^* = \arg \max_{\pi} \mathbb{E}_{\substack{\varphi \sim \xi, \\ \tau^\varphi \sim \pi | \varphi}} \left[\sum_{t=0}^{\infty} \gamma^t \mathbf{1}[q_t^\varphi \in \mathcal{F}_\varphi] \right].$$

Solutions to Problem 4.1 generally achieve a high probability of LTL satisfaction while being biased towards earlier satisfaction due to the discount factor γ . Details on product MDPs and Problem 4.1 can be found in Appendix C.

However, in a departure from existing literature, we will not assume that the set of atomic propositions is fixed between all LTL formulae for the same environment. Instead, we will assume that each LTL formula $\varphi \sim \xi$ has its own (finite) set of atomic propositions AP_φ . Accordingly, the alphabet $\Sigma_\varphi \subseteq 2^{AP_\varphi}$, assignments $\sigma^\varphi \in \Sigma_\varphi$, and labeling function $L_\varphi(s)$ are also conditioned on φ .

5. PlatoLTL

A key challenge in solving Problem 4.1 is how to condition the policy on a given LTL instruction φ . We build on recent approaches that learn a stationary policy π conditioned on the MDP state s and LDBA state q^φ (Jackermeier & Abate, 2025; Giuri et al., 2025). However, such approaches are designed for environments wherein all LTL specifications use the same set of atomic propositions, and do not scale well as the number of propositions is increased; we will see how PlatoLTL overcomes this challenge and achieves generalization through *parameterization*.

5.1. High-Level Overview

Figure 1 outlines our approach. We first train a policy π conditioned on arbitrary *reach-avoid sequences* of Boolean formulae of atomic propositions. To obtain a learned embedding of each sequence, PlatoLTL first meaningfully embeds its constituent propositions by reformulating them as instances of *atomic predicates*, and then builds the sequence embedding from the predicate instance embeddings. At evaluation time, given a new LTL specification φ , we construct the LDBA \mathcal{B}_φ , and extract a reach-avoid sequence of Boolean formulae corresponding to an accepting run from the initial LDBA state q_0^φ . Each Boolean formula in the sequence is associated with a transition in \mathcal{B}_φ , and succinctly represents the set of assignments that trigger that transition. This sequence is then used to condition the policy; if the LDBA state changes to a new state $q^{\varphi'}$, we compute a new accepting run from $q^{\varphi'}$ and condition the policy on the corresponding new sequence of Boolean formulae. Since the policy was trained on arbitrary sequences, it generalizes across LDBAs, and therefore across LTL formula structures.

5.2. Propositions as Predicate Instances

We assume that all atomic propositions used to compose our LTL formulae are instances drawn from a shared set of *atomic predicates*, Pred , which represent *parameterized* Boolean statements about the environment, such that the truth value depends on the input parameter values.

Given a set of parameters $x_f \in \mathcal{X}_f$, where $\mathcal{X}_f \subseteq \mathbb{R}^{n_f}$ is the n_f -dimensional parameter space for f , the mapping $f(x_f) : \mathcal{X}_f \rightarrow AP_\varphi$ instantiates atomic predicate $f \in \text{Pred}$ as an atomic proposition $p \in AP_\varphi$; thus $p = f(x_f)$ is a *predicate instance* of f . Our assumption is thus formalized as follows:

Assumption 5.1. Given formula $\varphi \sim \xi$, all atomic propositions $p \in AP_\varphi$ are such that $p = f(x_f)$ for some atomic predicate $f \in \text{Pred}$ and set of parameters $x_f \in \mathcal{X}_f$.

In other words, each atomic proposition in an LTL formula is equivalently a predicate instance with a particular set of fixed parameters.²

Example 5.2. An atomic proposition for entering a blue colored zone, $p = \text{at_blue}$, can be re-written as the predicate instance $p = \text{at}(0.0, 0.0, 1.0)$, where $f = \text{at}$ is the atomic predicate for entering a colored zone, and $x_f = (0.0, 0.0, 1.0)$ is the set of parameters representing “blue”.

Note that the parameter space \mathcal{X}_f can be a singleton, in which case f always creates the same proposition p as its only predicate instance: thus, Assumption 5.1 is compatible with atomic propositions (e.g., from standard LTL) that are not parameterized.

5.3. Embedding Predicate Instances

PlatoLTL computes embeddings $\phi(p)$ as follows:

1. The atomic proposition $p = f(x_f)$ is separated into its atomic predicate f and parameters x_f .
2. The predicate f is treated as a token and mapped to a learnable embedding $\phi_{\text{prd}}(f)$.
3. The parameters x_f are passed through a learnable, predicate-specific *parameter embedding network* $\rho_f(\cdot)$ to produce the parameter embedding $\rho_f(x_f)$.
4. The token and parameter embeddings are concatenated and passed through a learnable, predicate-specific *fusion network* $f_f(\cdot)$ to produce the final predicate instance embedding $\phi(p) = f_f(\phi_{\text{prd}}(f) \parallel \rho_f(x_f))$.

The fusion network thus acts as a learned transformation of the “base” predicate embedding, modulated by the parameters. We use a multilayer perceptron (MLP; Rumelhart et al., 1986) for the networks ρ_f and f_f .

²While not technically needed, for the benefit of interested readers Appendix D draws a connection between predicate instances and Plato’s Theory of Forms (Plato, 1992).

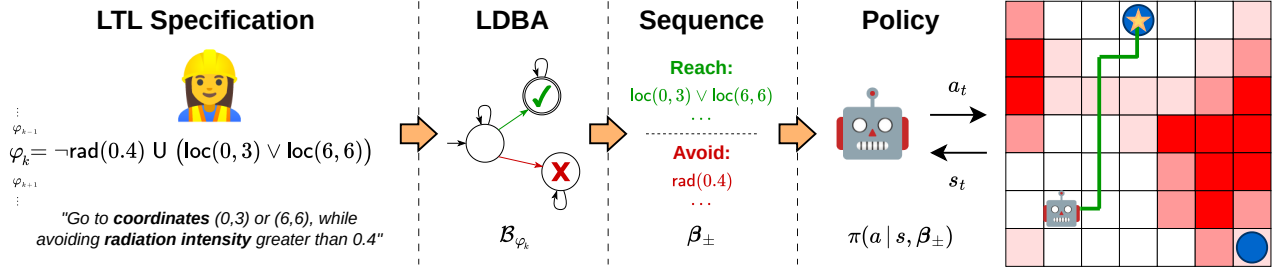


Figure 1. PlatoLTL overview. We first train a policy π conditioned on arbitrary *reach-avoid sequences* of Boolean formulae of propositions (corresponding to the second half of the diagram only). At evaluation time, given a new LTL specification φ , we construct an LDBA \mathcal{B}_φ representing the specification and extract a reach-avoid sequence of Boolean formulae to an accepting cycle in \mathcal{B}_φ upon which to condition the policy. Whenever the LDBA state changes, we re-condition the policy on a reach-avoid sequence from the new state. Since the policy was trained on arbitrary reach-avoid sequences, it generalizes across LDBAs, and therefore across LTL formula structures.

5.4. Composing Sequence Embeddings

The pyramid in Figure 2 illustrates the process of composing sequence embeddings. Given a reach-avoid sequence $\beta_\pm = \{(\beta_i^+, \beta_i^-)\}_{i=0}^{n-1}$, we first translate each Boolean formula β into an abstract syntax tree (AST), wherein the leaf nodes are propositions and internal nodes are logical operators. Each AST is treated as a directed graph, with edges from children to parent nodes, and leaf nodes are assigned embeddings $\phi(p)$ for their respective propositions while internal nodes are assigned learnable embeddings for their respective logical operators (which are treated as tokens).

We then apply a graph neural network (GNN; Zhou et al., 2020) to the graphs, and obtain the embeddings of the Boolean formulae as the final embeddings of the root nodes. We use a graph convolutional network (GCN; Kipf & Welling, 2017) for the GNN. We then concatenate the embeddings of β_i^+ and β_i^- at each step of the reach-avoid sequence, followed by applying a recurrent neural network (RNN; Sherstinsky, 2020) to the sequence back-to-front to obtain a single embedding. We use a gated recurrent unit (GRU; Cho et al., 2014) for the RNN.

5.5. Policy Architecture

Figure 2 illustrates the PlatoLTL policy architecture. The procedure described in Sections 5.3 and 5.4 represents the *sequence module* used to encode the reach-avoid sequence. We process observations from the environment using the *observation module*, which uses a convolutional neural network (CNN; LeCun et al., 1989) to process image-like features or an MLP for generic features. The outputs of both modules are then concatenated and passed into the *actor-critic* module, which uses an MLP to map from the joint task-observation embedding to a distribution over actions and a predicted value, thus completing the policy.

Following the approach taken by Hasanbeig et al. (2023), we handle ϵ -transitions in an LDBA by augmenting the action space of the policy with a special ϵ -action. For discrete

action spaces, the policy network outputs a categorical distribution with an additional logit for the ϵ -action, while for continuous action spaces the policy network outputs a mixed discrete-continuous distribution. Thus, the policy must learn to predict when to trigger the ϵ -transition. The probability of selecting the ϵ -action is set to 0 when no ϵ -transitions are available for the current LDBA state.

5.6. Training a Generalist Policy

Inspired by the approach of Jackermeier & Abate (2025), we train the policy end-to-end via goal-conditioned RL (Liu et al., 2022) using a generic training curriculum of increasingly challenging reach-avoid sequences, starting with one-step reach tasks and increasing to multi-step reach-avoid and reach-stay tasks by the final curriculum stage.

Let $\{(\beta_i^+, \beta_i^-)\}_{i=0}^{n-1}$ be an n -step reach-avoid sequence sampled from the curriculum; we assign a reward of $+1$ if the agent satisfies all formulae $\{\beta_i^+\}_{i=0}^{n-1}$ in sequence, we assign a reward of -1 if the agent satisfies the current β_i^- , and we assign a reward of 0 otherwise. We train the policy using Proximal Policy Optimization (PPO; Schulman et al., 2017).

Note that the reach-avoid sequences sampled for training are not tied to any particular LTL specification or LDBA, but rather represent the distribution of sequences that the agent is expected to encounter at evaluation time given LTL specification distribution ξ . As a result, the policy learns to generalize across LTL specifications at evaluation time.

5.7. Evaluation-Time Policy Execution

At evaluation time, given LDBA \mathcal{B}_φ and state q^φ , we perform a depth-first search (DFS) to obtain all possible paths to accepting cycles from q^φ , i.e., all accepting runs from q^φ (see Appendix E for details). For each accepting run $r^\varphi = (q^\varphi, q_1^\varphi, \dots)$ we then construct a sequence of Boolean

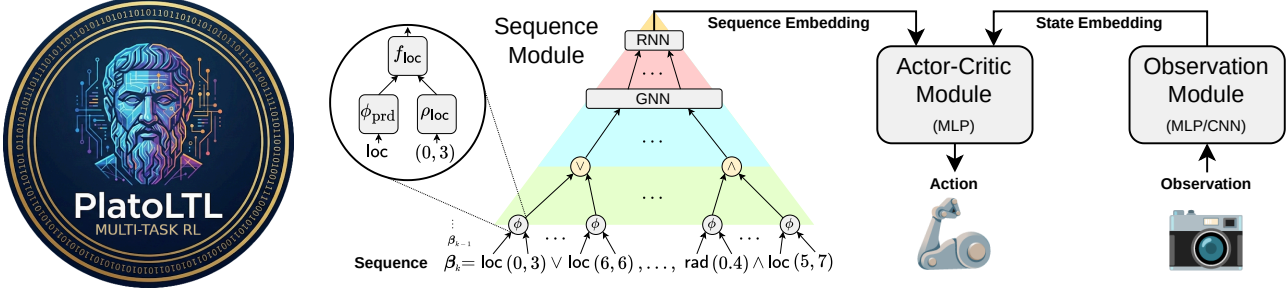


Figure 2. PlatoLTL policy architecture. The sequence module processes the given reach-avoid sequence of Boolean formulae into a learned sequence embedding. It first composes predicate instance embeddings using the predicate type and parameters for each proposition. It then builds up compositionally from the predicate instance embeddings, using a GNN over the Boolean formula graphs followed by an RNN over the sequence. The observation module processes the observation from the environment into a learned state embedding. The outputs are then concatenated and passed into the actor-critic module to obtain the action.

formulae $\beta_{\pm}^{\varphi} = ((\beta_0^{\varphi+}, \beta_0^{\varphi-}), (\beta_1^{\varphi+}, \beta_1^{\varphi-}), \dots)$ such that

$$\begin{aligned} \forall \sigma^{\varphi} \in \Sigma_{\varphi} : \sigma^{\varphi} \models \beta_i^{\varphi+} &\iff \delta_{\varphi}(q_i^{\varphi}, \sigma^{\varphi}) = q_{i+1}^{\varphi}, \\ \forall \sigma^{\varphi} \in \Sigma_{\varphi} : \sigma^{\varphi} \models \beta_i^{\varphi-} &\iff \delta_{\varphi}(q_i^{\varphi}, \sigma^{\varphi}) \notin \{q_i^{\varphi}, q_{i+1}^{\varphi}\}. \end{aligned}$$

In other words, $\beta_i^{\varphi+}$ represents the set of assignments that trigger the transition from q_i^{φ} to q_{i+1}^{φ} , while $\beta_i^{\varphi-}$ represents the set of assignments that would trigger a transition to any other state (excluding self-loops). Sequence β_{\pm}^{φ} thus represents a reach-avoid sequence of Boolean formulae to achieve accepting run r^{φ} . We use elementary *formula templates* to automatically construct minimally-sized $\beta_i^{\varphi+}$ and $\beta_i^{\varphi-}$; see Appendix F for details.

However, in general there may be more than one reach-avoid sequence extracted from the DFS, in which case the policy must choose which sequence to pursue. We use the learned value function (or ‘‘critic’’) of the policy to select the optimal sequence. The value function is an approximate lower bound on the discounted probability of LTL satisfaction, and thus choosing the reach-avoid sequence that maximizes critic value also maximizes (predicted) LTL satisfaction; see the work of Jackermeier & Abate (2025) for details.

Given the sequence-conditioned policy $\pi(a | s, \beta_{\pm})$, LDBA \mathcal{B}_{φ} , product MDP state (s, q^{φ}) , and set of reach-avoid sequences $RA_{q^{\varphi}} = \{\beta_{\pm}^{\varphi}\}_{q^{\varphi}}$ from LDBA state q^{φ} extracted from the DFS, we select the optimal reach-avoid sequence

$$\beta_{\pm}^{\varphi*} = \arg \max_{\beta_{\pm}^{\varphi} \in RA_{q^{\varphi}}} V^{\pi}(s, \beta_{\pm}^{\varphi})$$

upon each update of the LDBA state.

6. Experiments

We conduct experiments to answer the following research questions: **(Q1)** How does PlatoLTL compare to state-of-the-art LTL-guided RL approaches for zero-shot generalization across LTL specifications when the set of possible

atomic propositions is *large*? **(Q2)** Can PlatoLTL zero-shot generalize to atomic propositions *unseen* during training? **(Q3)** Can PlatoLTL generalize across an *infinite* number of atomic propositions?

6.1. Baselines

We compare PlatoLTL to two state-of-the-art approaches for zero-shot, multi-task LTL-guided RL, both of which construct an LDBA and extract reach-avoid sequences. DeepLTL (Jackermeier & Abate, 2025) conditions the policy directly on a sequence of sets of assignments, while LTL-GNN (Giuri et al., 2025) conditions the policy on a sequence of Boolean formulae, as in PlatoLTL. However, unlike PlatoLTL, which learns a shared parameterized embedding for all instances of the same predicate, both baselines learn a separate embedding for every unique assignment or proposition. DeepLTL has been demonstrated to significantly outperform previous methods such as LTL2Action (Vaezipoor et al., 2021) and GCRL-LTL (Qiu et al., 2023), which are thus omitted from our comparisons.

We do not include existing approaches that consider parameterization of LTL specifications, since they are either single-task and append the parameters to the observation space (Jothimurugan et al., 2019; 2021; Shukla et al., 2024) or are too restrictive to express arbitrary specifications; for example, SIAMS (Hatanaka et al., 2025) assumes a single parameter set per sequence step, restricting the task space to sequential reach tasks of one proposition each. Nor do we include GenZ-LTL (Guo et al., 2025), which enables generalization across propositions by remapping components of environment observations to generic ‘‘reach’’ and ‘‘avoid’’ observations, but relies on the assumption that the observation space can be partitioned into $2^{|AP_{\varphi}|}$ proposition-specific observations, produced by identical observation functions under output transformation; this assumption does not hold for the general environments that are considered to demonstrate the core features of the method in this paper.

6.2. Environments

Environments from existing literature use a small set of atomic propositions shared by all LTL specifications. Since PlatoLTL removes the need for this restriction, we introduce two novel environments, covering a diverse range of state and action spaces as well as atomic propositions.

The continuous *RGBZoneEnv* environment expands upon the *ZoneEnv* environment introduced by Vaezipoor et al. (2021), and requires a 2D point agent to navigate between a collection of colored zones, with zone colors resampled from across the RGB spectrum upon each environment reset. Atomic propositions are drawn from the predicate $\text{at}(r, g, b)$ for entering a colored zone with RGB value (r, g, b) . To observe zones, the agent has a *single* LiDAR that returns the distance and RGB value of the closest zone in each bin; essentially, a 1-dimensional RGB-D camera.

Meanwhile, the discrete *FalloutWorld* environment expands upon Vaezipoor et al. (2021)’s *LetterWorld* environment and requires a 2D grid-based agent to navigate between a collection of grid coordinates while not exceeding the permitted exposure to a hazardous radiation field; both the grid coordinates and radiation field are resampled upon each environment reset. Atomic propositions are drawn from the predicates $\text{loc}(x, y)$ for entering the grid coordinate (x, y) , and $\text{rad}(tol)$ for exceeding the radiation intensity threshold tol . To observe grid coordinates, the agent receives a *single* top-down image encoding only its own location. It also receives a top-down image of the radiation field intensities.

Note that both environments admit a very large or even *infinite* number of possible atomic propositions; *RGBZoneEnv* admits a continuous spectrum of colors, while *FalloutWorld* admits a continuous range of radiation intensity thresholds (as well as the discrete range of grid locations). Note also that neither observation space can be partitioned into $2^{|AP_\varphi|}$ proposition-specific observations from identical observation functions under output transformation. Further details on the environments can be found in Appendix G.1.

6.3. LTL Specifications

We evaluate the trained policy on a variety of LTL specifications, constructed from valid atomic propositions given the reset environment configuration. *Reach-avoid* specifications represent a sequence of one or more subgoals in which the agent must reach some atomic propositions while avoiding others. Meanwhile, *complex* specifications cover more advanced (and environment-specific) behaviors including reachability, safety, recurrence, persistence, and combinations thereof, and include both finite-horizon and infinite-horizon specifications. Details on the specifications used for evaluation can be found in Appendix G.2.

6.4. Evaluation Protocol

All methods are trained with the same curriculum, for 100M environment interactions in *RGBZoneEnv* and 50M in *FalloutWorld*; training hyperparameters are provided in Appendix G.3, while the training curriculum for each environment can be found in Appendix G.4. Since the baseline environments require a finite number of known possible atomic propositions, we train and evaluate on a large yet finite set of propositions; we use 1331 unique training propositions for *RGBZoneEnv*, and 228 for *FalloutWorld*. We also evaluate PlatoLTL on another large yet finite set of propositions unseen during training; 1000 for *RGBZoneEnv* and 226 for *FalloutWorld*. Finally, we both train and evaluate PlatoLTL on a continuous (i.e., infinite) set of propositions for each environment. For details regarding the training and evaluation propositions, see Appendix G.5.

For *reach-avoid* specifications we report success rate and average episode length over the number of environment interactions. For *complex* specifications, we report the success rate (SR) and average number of steps to satisfy the task (μ) for finite-horizon tasks φ , and average number of visits (AV) to accepting states for infinite-horizon tasks ψ . Results are averaged over 5 random seeds.

7. Results & Discussion

Figure 3 illustrates evaluation curves for *reach-avoid* tasks during training, and Tables 1 and 2 present evaluation results for *complex* tasks, for both environments. See Appendix H for visualizations of example trajectories with PlatoLTL.

Q1. From Figure 3, we see that PlatoLTL quickly converges to high success rate (98% for *RGBZoneEnv*, 93% for *FalloutWorld*) and low average episode length (~ 170 steps for *RGBZoneEnv*, ~ 65 steps for *FalloutWorld*). The baselines converge more slowly; this difference in convergence rate is moderate in *FalloutWorld*, and substantial in *RGBZoneEnv*, due to the latter using roughly 5 times as many propositions. As a result of earlier convergence, we see that PlatoLTL broadly achieves superior performance in Tables 1 and 2.

The ablation study in Appendix I.1 investigates the rate of convergence of each method over an increasing number of training propositions, while Appendix I.2 presents the performance of the baselines at convergence. In general, we find that as the number of training propositions increases, the performance at convergence remains similar for all three methods, but the rate of convergence decreases steadily for the baselines (to the point where convergence requires an impractically long training time when the number of propositions is large) while PlatoLTL is robust to this increase and remains unaffected. This is because the baseline approaches must learn a unique token embedding from scratch for each atomic proposition, while PlatoLTL learns a single

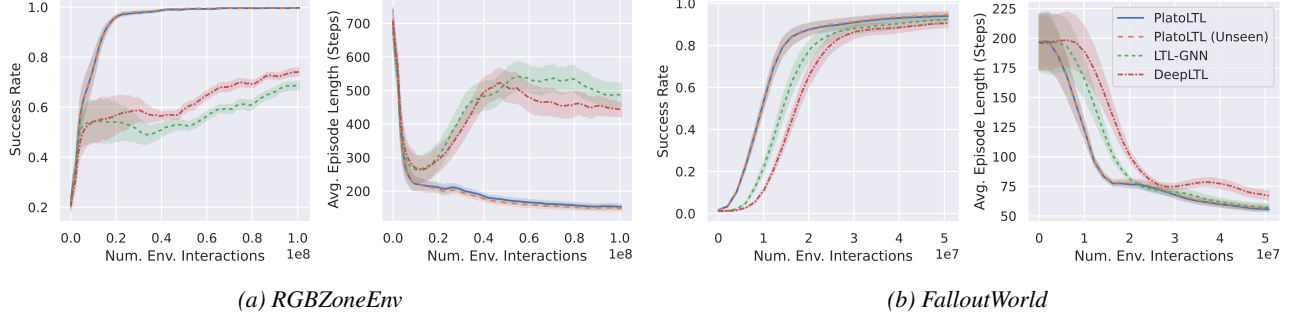


Figure 3. Success rate (as a proportion of total roll-outs) and average episode length (in steps) during training for *reach-avoid* LTL specifications composed from the training set of atomic propositions. Results are averaged over 5 seeds, 50 specifications per seed and 16 episodes per specification per seed, with 95% confidence intervals marked by the shaded area.

Table 1. Success rates (SR, in %) and average episode lengths (μ , in steps) for *complex* finite-horizon LTL specifications φ , composed from discrete sets of training propositions, for *RGBZoneEnv* (RGB) and *FalloutWorld* (FW). Also included for PlatoLTL are results for unseen and continuous sets of propositions. Results are averaged over 5 seeds and 512 episodes per seed, with ± 1 standard deviation.

	DEEPLTL		LTL-GNN		PLATO LTL		PLATO LTL (UNSEEN)		PLATO LTL (CONTINUOUS)		
	φ	SR (\uparrow)	μ (\downarrow)	SR (\uparrow)	μ (\downarrow)	SR (\uparrow)	μ (\downarrow)	SR (\uparrow)	μ (\downarrow)	SR (\uparrow)	
RGB	φ_1	77.2 \pm 16.5	389.75 \pm 44.51	66.4 \pm 14.2	401.63 \pm 24.18	99.8 \pm 0.2	179.47 \pm 3.67	99.8 \pm 0.2	179.74 \pm 5.20	99.7 \pm 0.2	172.85 \pm 2.32
	φ_2	72.0 \pm 15.6	383.26 \pm 35.11	65.7 \pm 9.2	406.22 \pm 32.09	98.9 \pm 0.6	185.51 \pm 8.82	99.5 \pm 0.3	180.92 \pm 3.46	98.9 \pm 0.5	180.33 \pm 2.68
	φ_3	85.0 \pm 14.6	312.17 \pm 49.46	75.7 \pm 14.9	352.44 \pm 50.73	100.0 \pm 0.0	154.94 \pm 2.13	99.8 \pm 0.1	155.17 \pm 3.88	99.8 \pm 0.1	152.25 \pm 1.46
	φ_4	58.1 \pm 9.1	255.83 \pm 15.79	58.6 \pm 6.7	253.74 \pm 17.48	97.4 \pm 1.1	124.92 \pm 2.61	98.4 \pm 0.5	125.49 \pm 3.16	98.0 \pm 0.6	122.01 \pm 2.60
	φ_5	73.1 \pm 8.8	253.69 \pm 25.95	76.3 \pm 2.5	241.23 \pm 10.32	98.5 \pm 0.6	116.99 \pm 4.80	98.5 \pm 0.4	114.22 \pm 4.31	98.6 \pm 0.3	111.99 \pm 2.90
	φ_6	76.2 \pm 7.1	163.54 \pm 15.46	82.0 \pm 1.5	157.32 \pm 9.14	99.6 \pm 0.3	67.24 \pm 3.54	99.7 \pm 0.3	68.29 \pm 3.20	99.6 \pm 0.3	67.63 \pm 2.49
FW	φ_7	96.2 \pm 0.8	73.58 \pm 2.77	96.9 \pm 0.4	62.52 \pm 0.77	98.6 \pm 0.6	61.23 \pm 2.15	97.6 \pm 0.5	62.06 \pm 1.34	98.7 \pm 0.5	62.20 \pm 2.40
	φ_8	84.5 \pm 2.1	53.49 \pm 3.30	87.4 \pm 0.7	48.48 \pm 1.52	91.2 \pm 1.2	48.88 \pm 1.21	90.4 \pm 1.4	49.14 \pm 1.90	89.3 \pm 1.1	47.54 \pm 2.32
	φ_9	79.6 \pm 3.6	63.87 \pm 5.09	93.7 \pm 1.0	46.81 \pm 1.02	96.6 \pm 0.9	41.79 \pm 2.09	95.7 \pm 0.6	43.10 \pm 1.63	96.1 \pm 1.1	44.17 \pm 1.72
	φ_{10}	89.8 \pm 0.9	49.72 \pm 2.68	91.0 \pm 0.8	45.57 \pm 1.26	93.5 \pm 0.4	44.70 \pm 1.34	92.3 \pm 0.9	43.84 \pm 1.60	92.9 \pm 1.4	44.45 \pm 2.10
	φ_{11}	77.0 \pm 2.6	70.46 \pm 3.51	90.3 \pm 1.7	52.92 \pm 2.12	95.1 \pm 1.3	47.28 \pm 2.33	95.2 \pm 1.4	49.64 \pm 1.80	93.6 \pm 1.3	48.48 \pm 1.70
	φ_{12}	97.5 \pm 0.9	27.12 \pm 1.09	98.6 \pm 0.1	24.72 \pm 0.48	99.0 \pm 0.1	23.45 \pm 0.66	99.3 \pm 0.3	24.05 \pm 0.53	98.8 \pm 0.4	24.19 \pm 1.02

Table 2. Average visits of the accepting LDBA state (AV, in steps) for *complex* infinite-horizon LTL specifications ψ , composed from discrete sets of training propositions, for *RGBZoneEnv* (RGB) and *FalloutWorld* (FW). Also included for PlatoLTL are results for unseen and continuous sets of propositions. Results are averaged over 5 seeds and 512 episodes per seed, with ± 1 standard deviation.

ψ	DEEPLTL	LTL-GNN	PLATO LTL	PLATO LTL (UNSEEN)	PLATO LTL (CONTINUOUS)	
RGB	ψ_1	101.46 \pm 117.87	22.65 \pm 12.83	783.16 \pm 72.31	792.79 \pm 62.59	777.23 \pm 32.86
	ψ_2	77.65 \pm 91.53	13.11 \pm 9.12	681.61 \pm 46.45	690.20 \pm 54.29	683.37 \pm 12.72
	ψ_3	81.32 \pm 96.73	20.10 \pm 7.54	781.07 \pm 63.06	787.79 \pm 60.37	771.62 \pm 38.85
	ψ_4	76.81 \pm 86.08	18.89 \pm 5.45	775.60 \pm 59.25	785.77 \pm 58.99	772.49 \pm 37.09
	ψ_5	2.46 \pm 0.87	2.16 \pm 0.61	7.33 \pm 0.16	7.35 \pm 0.16	7.73 \pm 0.15
	ψ_6	0.84 \pm 0.32	0.77 \pm 0.14	4.25 \pm 0.23	4.35 \pm 0.26	4.54 \pm 0.15
FW	ψ_7	277.59 \pm 4.28	287.55 \pm 6.59	290.74 \pm 3.20	291.62 \pm 2.80	290.97 \pm 2.08
	ψ_8	219.15 \pm 9.91	244.13 \pm 3.89	237.20 \pm 21.05	238.18 \pm 11.22	246.20 \pm 4.39
	ψ_9	198.05 \pm 13.79	185.72 \pm 7.73	155.12 \pm 21.52	153.33 \pm 18.55	141.88 \pm 12.16
	ψ_{10}	5.83 \pm 0.58	7.55 \pm 0.22	7.71 \pm 0.19	7.57 \pm 0.14	7.59 \pm 0.79
	ψ_{11}	4.35 \pm 0.64	5.02 \pm 0.53	4.32 \pm 0.63	4.06 \pm 0.61	4.31 \pm 0.59
	ψ_{12}	3.08 \pm 0.34	4.35 \pm 0.09	3.72 \pm 0.16	3.71 \pm 0.12	3.74 \pm 0.41

parameterized embedding for each predicate.

Q2 & Q3. From Figure 3, we see that PlatoLTL’s performance on unseen propositions remains at parity to that on training propositions, for both environments. This is corroborated by the results in Tables 1 and 2, which show that PlatoLTL achieves strong performance on both the finite set of unseen propositions and the continuous set of proposi-

tions, in line with that for the training propositions. This is because PlatoLTL learns the underlying structure relating the propositions, thus facilitating generalization; Appendix I.3 demonstrates that the baselines fail to generalize to unseen propositions, and Appendix I.1 shows that training performance of the baselines on a finite discretization of the continuous proposition space scales poorly as resolution increases. Indeed, PlatoLTL learns individual geometries for each predicate, placing them in separate parts of the embedding space; Appendix I.4 confirms this through a principal component analysis. Finally, Appendix I.5 investigates the number of training propositions required for generalization.

8. Conclusion

We have presented PlatoLTL, a novel LTL-guided RL approach that zero-shot generalizes both *compositionally* across LTL formula structures, and *parameterically* across atomic propositions. While the parameterizations studied in this paper are relatively straightforward, this is not unrealistic for real applications such as robotics, e.g., commanding an end-effector to move to position (x, y, z) in space. Future work would investigate more advanced and abstract parameterizations, e.g., parameterizing objects to pick/place by their latent representations from a pre-trained encoder.

Impact Statement

This paper presents work whose goal is to advance the field of Machine Learning. There are many potential societal consequences of our work, none which we feel must be specifically highlighted here.

References

Baier, C. and Katoen, J.-P. *Principles of model checking*. The MIT Press, Cambridge, Massachusetts London, England, 2008.

Bozkurt, A. K., Wang, Y., Zavlanos, M. M., and Pajic, M. Control Synthesis from Linear Temporal Logic Specifications using Model-Free Reinforcement Learning. In *2020 IEEE International Conference on Robotics and Automation (ICRA)*, pp. 10349–10355, Paris, France, May 2020. IEEE.

Bradbury, J., Frostig, R., Hawkins, P., Johnson, M. J., Leary, C., Maclaurin, D., Necula, G., Paszke, A., VanderPlas, J., Wanderman-Milne, S., and Zhang, Q. JAX: composable transformations of Python+NumPy programs, 2018.

Büchi, J. R. Symposium on Decision Problems: On a Decision Method in Restricted Second Order Arithmetic. In Nagel, E., Suppes, P., and Tarski, A. (eds.), *Logic, Methodology and Philosophy of Science*, volume 44 of *Studies in Logic and the Foundations of Mathematics*, pp. 1–11. Elsevier, 1966. ISSN: 0049-237X.

Cai, M., Hasanbeig, M., Xiao, S., Abate, A., and Kan, Z. Modular Deep Reinforcement Learning for Continuous Motion Planning With Temporal Logic. *IEEE Robotics and Automation Letters*, 6(4):7973–7980, October 2021.

Camacho, A., Toro Icarte, R., Klassen, T. Q., Valenzano, R., and McIlraith, S. A. LTL and Beyond: Formal Languages for Reward Function Specification in Reinforcement Learning. In *Proceedings of the Twenty-Eighth International Joint Conference on Artificial Intelligence*, pp. 6065–6073, Macao, China, August 2019. International Joint Conferences on Artificial Intelligence Organization.

Cho, K., Van Merriënboer, B., Bahdanau, D., and Bengio, Y. On the Properties of Neural Machine Translation: Encoder–Decoder Approaches. In *Proceedings of SSST-8, Eighth Workshop on Syntax, Semantics and Structure in Statistical Translation*, pp. 103–111, Doha, Qatar, 2014. Association for Computational Linguistics.

Giuri, M., Jackermeier, M., and Abate, A. Zero-Shot Instruction Following in RL via Structured LTL Representations. In *ICML 2025 Workshop on Programmatic Representations for Agent Learning*, 2025.

Guo, Z., Işık, İ., Ahmad, H. M. S., and Li, W. One Subgoal at a Time: Zero-Shot Generalization to Arbitrary Linear Temporal Logic Requirements in Multi-Task Reinforcement Learning. In *The Thirty-ninth Annual Conference on Neural Information Processing Systems*, 2025.

Hahn, E. M., Perez, M., Schewe, S., Somenzi, F., Trivedi, A., and Wojtczak, D. Omega-Regular Objectives in Model-Free Reinforcement Learning. In Vojnar, T. and Zhang, L. (eds.), *Tools and Algorithms for the Construction and Analysis of Systems - 25th International Conference*, volume 11427 of *Lecture Notes in Computer Science*, pp. 395–412. Springer, 2019.

Hasanbeig, H., Kroening, D., and Abate, A. Certified reinforcement learning with logic guidance. *Artificial Intelligence*, 322:103949, September 2023.

Hasanbeig, M., Kroening, D., and Abate, A. Deep Reinforcement Learning with Temporal Logics. In Bertrand, N. and Jansen, N. (eds.), *Formal Modeling and Analysis of Timed Systems*, volume 12288, pp. 1–22. Springer International Publishing, Cham, 2020. Series Title: Lecture Notes in Computer Science.

Hatanaka, W., Yamashina, R., and Matsubara, T. Reinforcement Learning of Flexible Policies for Symbolic Instructions With Adjustable Mapping Specifications. *IEEE Robotics and Automation Letters*, 10(3):2614–2621, March 2025.

Icarte, R. T., Klassen, T., Valenzano, R., and McIlraith, S. Using Reward Machines for High-Level Task Specification and Decomposition in Reinforcement Learning. In Dy, J. and Krause, A. (eds.), *Proceedings of the 35th International Conference on Machine Learning*, volume 80 of *Proceedings of Machine Learning Research*, pp. 2107–2116. PMLR, July 2018.

Icarte, R. T., Klassen, T. Q., Valenzano, R., and McIlraith, S. A. Reward Machines: Exploiting Reward Function Structure in Reinforcement Learning. *Journal of Artificial Intelligence Research*, 73:173–208, January 2022.

Jackermeier, M. and Abate, A. DeepLTL: Learning to Efficiently Satisfy Complex LTL Specifications for Multi-Task RL. In *The Thirteenth International Conference on Learning Representations, ICLR 2025, Singapore, April 24-28, 2025*, 2025.

Jothimurugan, K., Alur, R., and Bastani, O. A Composable Specification Language for Reinforcement Learning Tasks. In Wallach, H., Larochelle, H., Beygelzimer, A., Alché-Buc, F. d., Fox, E., and Garnett, R. (eds.), *Advances in Neural Information Processing Systems*, volume 32. Curran Associates, Inc., 2019.

Jothimurugan, K., Bansal, S., Bastani, O., and Alur, R. Compositional Reinforcement Learning from Logical Specifications. In Ranzato, M., Beygelzimer, A., Dauphin, Y., Liang, P. S., and Vaughan, J. W. (eds.), *Advances in Neural Information Processing Systems*, volume 34, pp. 10026–10039. Curran Associates, Inc., 2021.

Kingma, D. P. and Ba, J. Adam: A Method for Stochastic Optimization, 2014. Version Number: 9.

Kipf, T. N. and Welling, M. Semi-Supervised Classification with Graph Convolutional Networks. In *5th International Conference on Learning Representations, ICLR 2017, Toulon, France, April 24-26, 2017, Conference Track Proceedings*. OpenReview.net, 2017.

Křetínský, J., Meggendorfer, T., Sickert, S., and Ziegler, C. Rabinizer 4: From LTL to Your Favourite Deterministic Automaton. In Chockler, H. and Weissenbacher, G. (eds.), *Computer Aided Verification*, volume 10981, pp. 567–577. Springer International Publishing, Cham, 2018. Series Title: Lecture Notes in Computer Science.

LeCun, Y., Boser, B., Denker, J. S., Henderson, D., Howard, R. E., Hubbard, W., and Jackel, L. D. Backpropagation Applied to Handwritten Zip Code Recognition. *Neural Computation*, 1(4):541–551, December 1989.

León, B. G., Shanahan, M., and Belardinelli, F. In a Nutshell, the Human Asked for This: Latent Goals for Following Temporal Specifications. In *The Tenth International Conference on Learning Representations, ICLR 2022, Virtual Event, April 25-29, 2022*. OpenReview.net, 2022.

Liu, M., Zhu, M., and Zhang, W. Goal-Conditioned Reinforcement Learning: Problems and Solutions. In *Proceedings of the Thirty-First International Joint Conference on Artificial Intelligence*, pp. 5502–5511, Vienna, Austria, July 2022. International Joint Conferences on Artificial Intelligence Organization.

Manna, Z. and Pnueli, A. A hierarchy of temporal properties. In *Proceedings of the Ninth Annual ACM Symposium on Principles of Distributed Computing*, PODC ’90, pp. 377–410, New York, NY, USA, 1990. Association for Computing Machinery. event-place: Quebec City, Quebec, Canada.

Plato. *Republic*. Hackett Publishing, Indianapolis, 1992.

Pnueli, A. The temporal logic of programs. In *18th Annual Symposium on Foundations of Computer Science (sfcs 1977)*, pp. 46–57, Providence, RI, USA, September 1977. IEEE.

Qiu, W., Mao, W., and Zhu, H. Instructing Goal-Conditioned Reinforcement Learning Agents with Temporal Logic Objectives. In Oh, A., Naumann, T., Globerson, A., Saenko, K., Hardt, M., and Levine, S. (eds.), *Advances in Neural Information Processing Systems*, volume 36, pp. 39147–39175. Curran Associates, Inc., 2023.

Rumelhart, D. E., Hinton, G. E., and Williams, R. J. Learning representations by back-propagating errors. *Nature*, 323(6088):533–536, October 1986.

Schulman, J., Wolski, F., Dhariwal, P., Radford, A., and Klimov, O. Proximal Policy Optimization Algorithms, 2017. Version Number: 2.

Shah, A., Voloshin, C., Yang, C., Verma, A., Chaudhuri, S., and Seshia, S. A. LTL-Constrained Policy Optimization with Cycle Experience Replay. *Transactions on Machine Learning Research*, 2025.

Sherstinsky, A. Fundamentals of Recurrent Neural Network (RNN) and Long Short-Term Memory (LSTM) network. *Physica D: Nonlinear Phenomena*, 404:132306, March 2020.

Shukla, Y., Burman, T., Kulkarni, A. N., Wright, R., Velasquez, A., and Sinapov, J. Logical Specifications-guided Dynamic Task Sampling for Reinforcement Learning Agents. *Proceedings of the International Conference on Automated Planning and Scheduling*, 34:532–540, May 2024.

Sickert, S., Esparza, J., Jaax, S., and Křetínský, J. Limit-Deterministic Büchi Automata for Linear Temporal Logic. In Chaudhuri, S. and Farzan, A. (eds.), *Computer Aided Verification*, volume 9780, pp. 312–332. Springer International Publishing, Cham, 2016. Series Title: Lecture Notes in Computer Science.

Sutton, R. S. and Barto, A. *Reinforcement learning: an introduction*. Adaptive computation and machine learning. The MIT Press, Cambridge, Massachusetts, nachdruck edition, 2014.

Vaezipoor, P., Li, A. C., Icarte, R. T., and McIlraith, S. A. LTL2Action: Generalizing LTL Instructions for Multi-Task RL. In *Proceedings of the 38th International Conference on Machine Learning, ICML*, volume 139 of *Proceedings of Machine Learning Research*, pp. 10497–10508, 2021.

Voloshin, C., Verma, A., and Yue, Y. Eventual discounting temporal logic counterfactual experience replay. In *Proceedings of the 40th International Conference on Machine Learning, ICML’23*. JMLR.org, 2023. Place: Honolulu, Hawaii, USA.

Xu, D. and Fekri, F. Generalization of temporal logic tasks via future dependent options. *Machine Learning*, 113(10):7509–7540, October 2024.

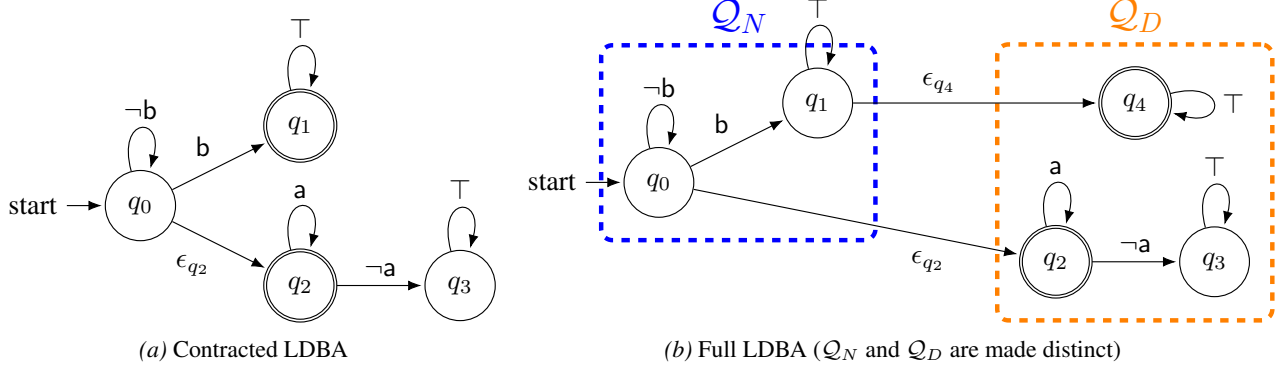
Yalcinkaya, B., Lauffer, N., Vazquez-Chanlatte, M., and Seshia, S. A. Compositional Automata Embeddings for Goal-Conditioned Reinforcement Learning. In Glocer-
sons, A., Mackey, L., Belgrave, D., Fan, A., Paquet, U., Tomczak, J. M., and Zhang, C. (eds.), *Advances in Neural Information Processing Systems 38: Annual Conference on Neural Information Processing Systems 2024, NeurIPS 2024, Vancouver, BC, Canada, December 10 - 15, 2024*, 2024.

Yuan, L. Z., Hasanbeig, M., Abate, A., and Kroening, D. Modular Deep Reinforcement Learning with Temporal Logic Specifications, 2019. Version Number: 2.

Zhang, H., Wang, H., and Kan, Z. Exploiting Transformer in Sparse Reward Reinforcement Learning for Interpretable Temporal Logic Motion Planning. *IEEE Robotics and Automation Letters*, 8(8):4831–4838, August 2023.

Zhang, H., Wang, H., Huang, X., Chen, W., and Kan, Z. Exploiting Hybrid Policy in Reinforcement Learning for Interpretable Temporal Logic Manipulation. In *2024 IEEE/RSJ International Conference on Intelligent Robots and Systems (IROS)*, pp. 13795–13800, Abu Dhabi, United Arab Emirates, October 2024. IEEE.

Zhou, J., Cui, G., Hu, S., Zhang, Z., Yang, C., Liu, Z., Wang, L., Li, C., and Sun, M. Graph neural networks: A review of methods and applications. *AI Open*, 1:57–81, 2020.


 Figure 4. LDBA for the formula $(F G a) \vee F b$.

A. LTL Satisfaction Semantics

Let $w[i] = \sigma_i$ and $w[i\dots] = (\sigma_i, \sigma_{i+1}, \sigma_{i+2}, \dots)$. The satisfaction relation $w \models \varphi$ is recursively defined as follows (Baier & Katoen, 2008):

$$\begin{aligned}
 w \models \top & \\
 w \models p & \iff p \in w[0] \\
 w \models \varphi \wedge \psi & \iff w \not\models \varphi \\
 w \models \neg \varphi & \iff w \models \varphi \wedge w \models \psi \\
 w \models X \varphi & \iff w[1\dots] \models \varphi \\
 w \models \varphi U \psi & \iff \exists j \geq 0 \text{ s.t. } w[j\dots] \models \psi \wedge \forall 0 \leq i < j : w[i\dots] \models \varphi
 \end{aligned}$$

B. Illustrated Example of an LDBA

Figure 4a presents an LDBA for the formula $(F G a) \vee F b$, which expresses a persistence requirement and a reachability specification. The automaton starts in state q_0 and transitions to the accepting state q_1 upon observing proposition b . Once it has reached q_1 , it stays there indefinitely. This captures the $F b$ (eventually satisfy b) component of the specification. Alternatively, it can transition to the accepting state q_2 without consuming any input via the ϵ -transition ϵ_{q_2} . Once in q_2 , the automaton accepts exactly the words where a is true at every step. This captures the $F G a$ (eventually *always* satisfy a) component of the specification.

Note that Figure 4a presents a contracted (yet equivalent) version of the full LDBA that strictly follows the LDBA definition in Section 3.3. The full LDBA is illustrated in Figure 4b, with the initial component Q_N and accepting component Q_D made distinct. Note that this distinction is technically not possible in Figure 4a's contracted LDBA, yet the two automata are functionally equivalent since ϵ -transition ϵ_{q_4} is trivial; in other words, the contracted LDBA simply encodes that the automaton should *always* take ϵ -transition ϵ_{q_4} if possible.

This *LDBA contraction* is a practical optimization that removes all unnecessary ϵ -transitions, i.e., those corresponding to subformulae that do not require non-determinism (such as $F b$), and is done to reduce the number of nodes and edges while keeping LDBA behavior functionally equivalent. This helps to keep the reach-avoid sequences given to the agent as simple as possible, and also simplifies checking LTL satisfaction at run-time.

C. Product MDPs and Efficient LTL Satisfaction

Product MDPs are defined as follows:

Definition C.1 (Product MDP; Jackermeier & Abate, 2025). The *product MDP* \mathcal{M}^φ of an MDP \mathcal{M} and an LDBA \mathcal{B}_φ synchronizes the execution of \mathcal{M} and \mathcal{B}_φ . Formally, \mathcal{M}^φ is an MDP with state space $\mathcal{S}^\varphi = \mathcal{S} \times \mathcal{Q}_\varphi$, action space

$\mathcal{A}^\varphi = \mathcal{A} \cup \mathcal{E}_\varphi$, initial state distribution $\mu^\varphi(s, q^\varphi) = \mu(s) \cdot \mathbb{1}[q^\varphi = q_0^\varphi]$, and transition function

$$p^\varphi((s', q'^\varphi) | (s, q^\varphi), a) = \begin{cases} p(s' | s, a) & \text{if } a \in \mathcal{A} \wedge q'^\varphi = \delta_\varphi(q^\varphi, L_\varphi(s)), \\ 1 & \text{if } a = \epsilon_{q^\varphi} \wedge q'^\varphi = \delta_\varphi(q^\varphi, a) \wedge s' = s, \\ 0 & \text{else.} \end{cases}$$

Note that the action space in \mathcal{M}^φ is extended with \mathcal{E} to allow the policy to select ϵ -transitions in \mathcal{B}_φ without acting in the MDP. Trajectories in \mathcal{M}^φ are infinite sequences $\tau^\varphi = ((s_0, q_0^\varphi), a_0, (s_1, q_1^\varphi), a_1, \dots)$, and run $\tau_q^\varphi = (q_0^\varphi, q_1^\varphi, q_2^\varphi, \dots)$ is the projection of τ^φ onto \mathcal{B}_φ . We can thus restate the satisfaction probability of LTL formula φ in \mathcal{M}^φ as

$$P(\pi \models \varphi) = \mathbb{E}_{\tau^\varphi \sim \pi | \varphi} [\mathbb{1}[\inf(\tau_q^\varphi) \cap \mathcal{F}_\varphi \neq \emptyset]], \quad (2)$$

where $\inf(\tau_q^\varphi)$ is the set of states that occur infinitely often in τ_q^φ .

A proxy for maximizing Equation 2 is to reward the agent for visiting an accepting LDBA state in \mathcal{F}_φ as many times as possible, assigning a reward of +1 whenever $q_t^\varphi \in \mathcal{F}_\varphi$ and 0 otherwise. To ensure finite return, one can employ *eventual discounting* (Voloshin et al., 2023), only discounting time steps corresponding to visits to accepting LDBA states. The optimal policy under such a reward scheme yields an LTL satisfaction probability with a sub-optimality gap relative to the optimal policy in Equation 1 that is upper-bounded by a term logarithmic in the discount factor; see the work of Voloshin et al. (2023) for details.

However, eventual discounting does not consider the *efficiency* of LTL satisfaction, i.e., the number of time steps required to satisfy the LTL specification. To trade off between maximizing satisfaction probability and efficiency, we instead discount *all* time steps and solve Problem 4.1, which has been demonstrated to achieve a high probability of LTL satisfaction while being biased towards earlier satisfaction due to the discount factor γ .

D. Aside: Connection to Plato’s Theory of Forms

Anecdotally, it is often difficult to construct an LTL specification that accurately matches the desired task outcome, in particular those tasks originally defined in natural language. This is because natural language tasks tend to implicitly assume constraints, dependencies and edge cases that are imperfectly translated (or forgotten entirely) during the formulation of the LTL specification.

We can draw a connection to Plato’s Theory of Forms (Plato, 1992), wherein the ultimate “Form of the Good” (desired task outcome) is imperfectly represented as a combination of base concepts, or “Forms” (atomic predicates), which are instantiated as “particulars” (atomic propositions as predicate instances) to create an imperfect imitation of “Good” (the LTL specification).

While not scientifically relevant, we found this connection amusing and it inspired the name of our approach, and we believed it to be worthy of note.

E. Computing Paths to Accepting Cycles

The DFS algorithm to compute paths to accepting cycles is presented in Algorithm 1. Note that the reach-avoid sequences are infinite, and so we approximate the looping part of β_\pm^φ by truncation such that the truncated sequence visits an accepting state k times, where k is a hyperparameter (set to $k = 2$ for our experiments).

Furthermore, as noted by Jackermeier & Abate (2025), in practice it can prove too restrictive for the trained policy to avoid all LDBA states that are not the next state in the selected accepting run (or the current state). Therefore, we mark as “avoid” only those LDBA states that are *sink states* (from which there does not exist any valid path from a sink state to an accepting cycle) and those LDBA states that lead the agent back along the current path (and thus represent regressing back to an earlier stage of the task).

F. Boolean Formula Construction

It is possible to map a set of assignments into a disjunctive normal form (DNF) Boolean formula. However, the DNF formula is often large and complex, and we would prefer a succinct, semantically-meaningful representation that is as compact as

Algorithm 1 Computing paths to accepting cycles (Jackermeier & Abate, 2025)

Require: An LDBA $\mathcal{B} = \langle \mathcal{Q}, q_0, \Sigma, \delta, \mathcal{F}, \mathcal{E} \rangle$ and current state q .

```

1: function DFS( $q, p, i$ )  $\{i$  is the index of the last seen accepting state, or  $-1$  otherwise $\}$ 
2:    $P \leftarrow \emptyset$ 
3:   if  $q \in \mathcal{F}$  then
4:      $i \leftarrow |p|$ 
5:   end if
6:   for all  $\sigma \in \Sigma \cup \{\varepsilon\}$  do
7:      $p' \leftarrow [p, q]$ 
8:      $q' \leftarrow \delta(q, \sigma)$ 
9:     if  $q' \in p$  then
10:      if index of  $q'$  in  $p \leq i$  then
11:         $P = P \cup \{p'\}$ 
12:      end if
13:    else
14:       $P = P \cup \text{DFS}(q', p', i)$ 
15:    end if
16:   end for
17:   return  $P$ 
18: end function
19:  $i \leftarrow 0$  if  $q \in \mathcal{F}$  else  $i \leftarrow -1$ 
20: return DFS( $q, [], i$ )

```

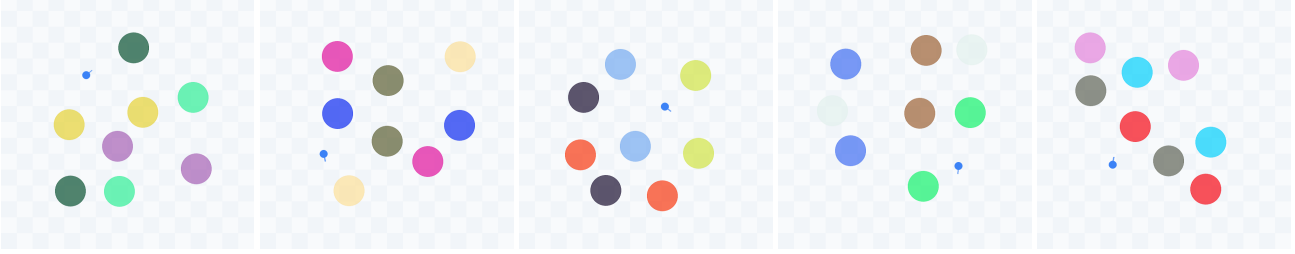
possible to minimize the support of the distribution over which our policy must generalize. Thus, we utilize elementary *formula templates* as a heuristic to construct minimally-sized $\beta_i^{\varphi+}$ and $\beta_i^{\varphi-}$.

Giuri et al. (2025) provide a comprehensive method for the construction of minimal Boolean formulae from sets of arbitrary assignments; such a method could indeed be applied in the case of PlatoLTL for arbitrary environments. However, for the experiments in this paper, we exploited the fact that, for both environments, each assignment corresponds to exactly one atomic proposition, with the exception of the assignment representing the empty set of propositions; i.e., no more than one proposition will be true at any given time. Thus, any set of assignments can simply be represented as an OR of propositions, and AST construction becomes trivial. If there is only one assignment, we omit the OR node, and if the set of assignments contains all propositions except p and also contains the assignment for the empty set of propositions (i.e., $\neg p$), then we omit the OR node and instead use a NOT node connected to the node for p . We emphasize that this simplification is not a limitation of PlatoLTL, but rather a convenience afforded by the nature of the environments used for experiments.

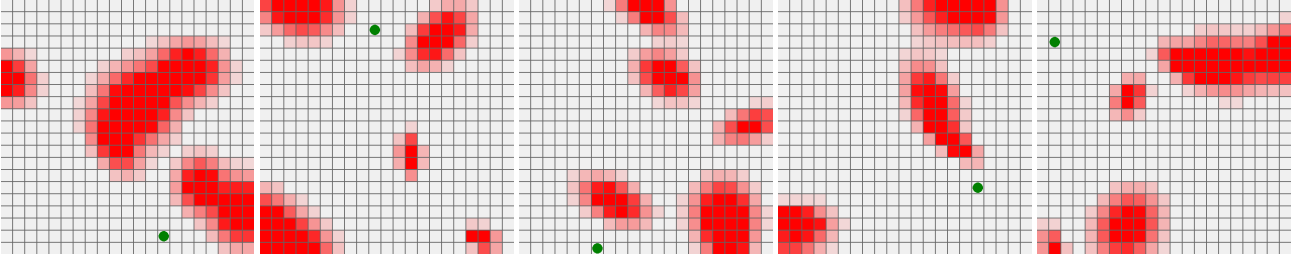
G. Experimental Details

G.1. Environments

RGBZoneEnv. The *RGBZoneEnv* environment consists of a bounded 2D plane containing a point agent and 8 colored zones (circular regions with fixed radius), grouped into four pairs, with each pair having a unique RGB value. The observation space principally consists of a 32-bin “RGB LiDAR” attached to the agent with 5 channels; the first three channels are the RGB value of the closest colored zone, the fourth channel is intensity $e^{-\alpha x}$, where x is Euclidean distance to the center of the closest colored zone and $\alpha = 0.5$ is a fixed gain, and the fifth channel is a Boolean flag indicating whether a zone is detected. The observation space also includes linear velocity and acceleration in the agent’s frame as well as angular velocity. The action space consists of the forward driving force and the turning velocity. All observations and actions are normalized to $[-1, 1]$ with the exception of the fifth RGB LiDAR channel which takes the values $\{0, 1\}$. The initial agent position and orientation and the zone locations are resampled uniformly from the environment space upon each reset, with a minimum distance between the agent and the zones (and between the zones) to prevent any overlap. Meanwhile, the RGB values of the zones are uniformly resampled from the RGB color space (or the finite set of colors selected for training/evaluation in experiments), with a minimum Euclidean distance in RGB color space between sampled colors. See Figure 5a for visualizations of the environment.



(a) *RGBZoneEnv*. The small blue circle denotes the agent position and orientation, and the colored circles represent the zones.



(b) *FalloutWorld*. The green circle denotes the agent location and the red patches illustrate the radiation field. Note that there are no goal locations; this is because information about the goal locations is found within the LTL specification, not the environment state or observations.

Figure 5. Visualizations of example environment reset configurations. In both cases, the distribution of environment resets covers an infinite number of possible atomic propositions, as described in Appendix G.5.

RGBZoneEnv has a single predicate type. The $\text{at}(r, g, b)$ predicate is true if the agent enters a colored zone with RGB value (r, g, b) , where $r, g, b \in [0, 1]$. Upon each environment reset, the colors for the predicate instances in the LTL specification are sampled from the zone RGB values in the environment.

FalloutWorld. The *FalloutWorld* environment consists of a 21×21 grid, containing the agent as well as a (potentially hazardous) continuous-valued radiation field. The observation space consists of a 21×21 image with two channels; the first is a one-hot encoding of the agent location with values $\{0, 1\}$, and the second is a map of the radiation intensity with values $[0, 1]$. The action space consists of 5 actions; moving up, down, left, right, and remaining stationary. The initial agent location and the radiation field are resampled upon each environment reset; the initial agent location is sampled uniformly from the grid space, and the radiation field is a (clipped and truncated) sum of anisotropic Gaussian functions with randomly sampled centers, standard deviations, rotations and amplitudes. See Figure 5b for visualizations of the environment.

FalloutWorld has two predicate types. The $\text{loc}(x, y)$ predicate is true if the agent enters the “goal” location (x, y) , where $x, y \in \{0, 1, \dots, 20\}$, and the $\text{rad}(tol)$ predicate is true if the agent enters a grid location with radiation intensity greater than the threshold $tol \in [0, 1]$. Upon each environment reset, validity checking is used to prevent impossible tasks; i.e., ensuring that the initial agent location and the specification-relevant goal locations are not at grid locations that exceed any specification-relevant radiation threshold, and that all specification-relevant goal locations are reachable from the initial location without exceeding any specification-relevant radiation threshold.

G.2. Evaluation LTL Specifications

Table 3 lists the template *reach-avoid* LTL specifications; 50 specifications randomly sampled from these templates were periodically evaluated over 16 episodes during training, with different predicate instances sampled for each episode according to the sampled environment configuration.

Tables 4a and 4b list the template *complex* finite-horizon and infinite-horizon specifications, respectively. Each of these template specifications were evaluated over 512 episodes, again with different predicate instances sampled for each episode.

Table 3. Template reach-avoid LTL specifications used for evaluation in *RGBZoneEnv* (RGB) and *FalloutWorld* (FW). The notation p_i represents the i -th predicate instance of atomic predicate p .

RGB $F(at_0 \wedge F(at_1 \wedge F(at_2)))$ $\neg at_0 \cup (at_1 \wedge (\neg at_2 \cup at_3))$	$F(loc_0 \wedge F(loc_1 \wedge F(loc_2)))$ $\neg rad_0 \cup (loc_0 \wedge (\neg rad_0 \cup loc_1))$ $\neg (rad_0 \vee loc_0) \cup (loc_1 \wedge (\neg (rad_0 \vee loc_0) \cup loc_2))$ $\neg (rad_0 \vee loc_0) \cup (loc_1 \wedge (\neg (rad_0 \vee loc_2) \cup loc_0))$
---	--

Table 4. Template complex LTL specifications used for evaluation in *RGBZoneEnv* (RGB) and *FalloutWorld* (FW). The notation p_i represents the i -th predicate instance of atomic predicate p .

(a) Finite-horizon specifications φ		(b) Infinite-horizon specifications ψ	
RGB	$\varphi_1 F(at_0 \wedge (\neg at_1 \cup at_2)) \wedge F at_3$	$\psi_1 FG at_0$	
	$\varphi_2 F at_0 \wedge (\neg at_0 \cup (at_1 \wedge F at_2))$	$\psi_2 FG at_0 \wedge F(at_1 \wedge F at_2)$	
	$\varphi_3 F(at_0 \vee at_1) \wedge F at_2 \wedge F at_3$	$\psi_3 FG at_0 \wedge G \neg at_1$	
	$\varphi_4 \neg(at_0 \vee at_1) \cup (at_2 \wedge F at_3)$	$\psi_4 G((at_0 \vee at_1) \Rightarrow F at_2) \wedge FG(at_0 \vee at_3)$	
	$\varphi_5 \neg at_0 \cup ((at_1 \vee at_2) \wedge (\neg at_0 \cup at_3))$	$\psi_5 GF at_0 \wedge GF at_1$	
	$\varphi_6 ((at_0 \vee at_1) \Rightarrow (\neg at_2 \cup at_3)) \cup at_2$	$\psi_6 GF at_0 \wedge GF at_1 \wedge GF at_2 \wedge G \neg at_3$	
FW	$\varphi_7 F(loc_0 \wedge (\neg rad_0 \cup loc_1)) \wedge F loc_2$	$\psi_7 FG \neg rad_0$	
	$\varphi_8 (\neg rad_0 \cup loc_0) \wedge (\neg loc_0 \cup loc_1)$	$\psi_8 FG \neg rad_0 \wedge F(loc_0 \wedge F loc_1)$	
	$\varphi_9 F(loc_0 \vee loc_1) \wedge (\neg rad_0 \cup loc_2)$	$\psi_9 G(rad_0 \Rightarrow F loc_0) \wedge F(loc_1 \wedge F loc_2)$	
	$\varphi_{10} \neg(rad_0 \vee loc_0) \cup (loc_1 \wedge F loc_2)$	$\psi_{10} GF loc_0 \wedge GF loc_1 \wedge G \neg rad_0$	
	$\varphi_{11} \neg rad_0 U ((loc_0 \vee loc_1) \wedge (\neg rad_0 \cup loc_2))$	$\psi_{11} GF loc_0 \wedge GF loc_1 \wedge F loc_2 \wedge G \neg rad_0$	
	$\varphi_{12} (rad_0 \Rightarrow (\neg loc_0 \cup (loc_1 \vee loc_2))) \cup loc_0$	$\psi_{12} GF loc_0 \wedge GF loc_1 \wedge G F loc_2$	

G.3. Training Hyperparameters

Neural networks. For all methods, we use an MLP for the actor-critic module, where both the actor and critic have hidden layer sizes [512, 512] and ReLU internal activations. In continuous environments such as *RGBZoneEnv*, the actor has a tanh output layer for the mean and standard deviation of a diagonal Gaussian distribution over the action space, and also outputs the log-probability of selecting the ϵ -action (which is only used if an ϵ -transition is available). In discrete environments such as *FalloutWorld*, the actor has a softmax output layer for the categorical distribution of size $|\mathcal{A}| + 1$, where the additional logit represents the ϵ -action. The critic outputs the predicted value of the value function.

For *RGBZoneEnv*, the observation module uses a 1D CNN for the RGB LiDAR observations, with [32, 64] channels, a kernel size of 5, a stride of 1, circular padding, and an average-pooling layer with stride and kernel size 2 after each convolution, and uses a linear layer of size 64 for the proprioceptive observations. The outputs of these networks are then concatenated and sent through a linear layer of size 512. For *FalloutWorld*, the observation module uses a 2D CNN, with [16, 32, 32, 64] channels, a kernel size of 5×5 for the first convolution and 3×3 for the rest, a stride of 2 in each direction for the first convolution and 1 for the rest, and no padding. In both cases, the observation module uses ReLU internal activations throughout.

For PlatoLTL, the sequence module uses predicate token embeddings of size 16 and a predicate-specific linear layer of size 16 to embed predicate parameters. These are concatenated and sent through a predicate-specific linear layer of size 32 to obtain proposition embeddings. For LTL-GNN (Giuri et al., 2025), we use proposition token embeddings of size 32. In both cases, we use a GCN with hidden layer sizes [64, 64] that outputs AST root embeddings of size 32. Meanwhile, for DeepLTL (Jackermeyer & Abate, 2025) we use assignment token embeddings of size 32 and an MLP with hidden layer sizes [64, 64] for network ρ . For all three methods we use a GRU network with a hidden layer of size 64, and the sequence modules have ReLU internal activations throughout.

Note that in all cases, the sequence module is much smaller than the observation and actor-critic models, with far fewer parameters; we observe that adding the capability to process complex sequences is often a relatively lightweight modification to a potentially large “standard” policy architecture.

PPO. The hyperparameters for PPO (Schulman et al., 2017) are listed for both environments in Table 5; all methods use the same hyperparameters. We use Adam (Kingma & Ba, 2014) for all experiments.

Table 5. Hyperparameters for PPO. Dashes (—) indicate the hyperparameter value is the same for both environments.

Parameter	RGBZoneEnv	FalloutWorld
Number of processes	128	—
Steps per process per update	1024	512
Epochs	5	4
Batch size	32768	4096
Discount factor	0.998	0.993
GAE- λ	0.95	—
Entropy coefficient	0.003	0.03
Value loss coefficient	0.5	—
Max gradient norm	1.0	—
Clipping (ϵ)	0.2	—
Adam learning rate	0.0005	—
Adam epsilon	1e-08	—

G.4. Training Curricula

We use training curricula to gradually introduce more challenging tasks during training, starting with one-step reach tasks and increasing to multi-step reach-avoid and reach-stay tasks by the final curriculum stage. Reach-avoid sequences take the form $\{(\beta_i^+, \beta_i^-)\}_{i=0}^{n-1}$, while reach-stay sequences take the form $((\epsilon, \beta_0^-), (p, \neg p))$. Table 6 details the training curricula for *RGBZoneEnv* and *FalloutWorld*. For both environments, Boolean formulae β are simple disjunctions of predicate instances, and valid predicate instance parameters are sampled based on the reset environment configuration.

RGBZoneEnv. For *RGBZoneEnv*, we use a curriculum similar to that used for *ZoneEnv* by [Jackermeier & Abate \(2025\)](#). The first four stages consist of reach-avoid sequences of increasing difficulty, and the final three stages are a mix of reach-avoid and reach-stay tasks.

FalloutWorld. For *FalloutWorld*, we use a curriculum similar to that for *RGBZoneEnv* for the *loc* predicate instances, but with the gradual addition of a *rad* predicate instance to the avoid sets. We found that keeping this probability at 0.0 for the first couple curriculum stages is crucial for efficient learning, since this allows the agent to freely explore and learn the association between its own location and the locations in the goal sequence without needing to be cautious about radiation.

However, unlike with *RGBZoneEnv*, we do not include reach-stay sequences for *loc* predicate instances in the curriculum; in practice, we found that the policy was unable to consistently complete such sequences (regardless of the LTL-guided RL method used), since taking even a single action different to the action for remaining stationary would immediately lead to failure. Instead, we consider reach-stay sequences for \neg *rad* predicate instances, i.e., $((\epsilon, \perp), (\neg \text{rad}, \text{rad}))$, representing that the agent must eventually avoid violating the radiation intensity threshold for all future time. This is reflected by the infinite-horizon LTL specifications in Appendix G.2, which include $\mathbf{F} \mathbf{G} \neg \text{rad}$ components but not $\mathbf{F} \mathbf{G} \text{loc}$ components.

G.5. Training and Evaluation Atomic Propositions

RGBZoneEnv. For *RGBZoneEnv*, we use the predicate instances $\text{at}(r, g, b)$ for each (r, g, b) point in the $11 \times 11 \times 11$ grid spanning the RGB color space (interval 0.1, offset 0.0 starting from the origin), for a total of 1331 unique training propositions. We also use $\text{at}(r, g, b)$ for the $10 \times 10 \times 10$ grid interleaved within the training grid (interval 0.1, offset 0.05 starting from the origin) for the unseen evaluation propositions, for a total of 1000 additional unique propositions. To obtain the continuous set of propositions, we uniformly sample (r, g, b) from the RGB color space. In all cases, we enforce a minimum distance in color space between sampled colors.

FalloutWorld. For *FalloutWorld*, we use the predicate instances $\text{loc}(x, y)$ for each (x, y) location in the 21×21 checkerboard spanning the grid, and the predicate instances $\text{rad}(tol)$ for each $tol \in \{0.2, 0.3, 0.4, 0.5, 0.6, 0.7, 0.8\}$, for a total of 228 unique training propositions. We also use each $\text{loc}(x, y)$ in the inverse of the checkerboard as well as $\text{rad}(tol)$ for each $tol \in \{0.25, 0.35, 0.45, 0.55, 0.65, 0.75\}$ for the unseen evaluation propositions, for a total of 226 additional unique propositions. To obtain the continuous set of propositions, we sample $tol \sim [0.2, 0.8]$; we also sample discrete (x, y) from all possible locations in the grid, noting that there is only a finite number of unique $\text{loc}(x, y)$ predicate instances.

Table 6. Curricula for training sequences. For each stage, we list the success rate threshold κ for progression (measured over a rolling window of the 128 latest episodes), the sequence type (reach-avoid/reach-stay), the probability P_{seq} of sampling a sequence of that type, the number of steps n in the sequence (or, for reach-stay tasks, the number of consecutive time steps for satisfying the “stay” sub-task), the numbers of at/loc predicate instances in each reach (β_i^+) and avoid (β_i^-) Boolean formula, and (for reach-avoid sequences in *FalloutWorld*) the probability P_{rad} of including a *rad* predicate instance in each β_i^- . Dashes (—) indicate “not applicable”.

STAGE	κ	TYPE	P_{seq}	n	$ \beta_i^+ $	$ \beta_i^- $	P_{rad}
RGBZONEENV	1	REACH-AVOID	1.0	1	1	0	—
	2	0.95	REACH-AVOID	1.0	2	1	0
	3	0.95	REACH-AVOID	1.0	1	1	—
	4	0.95	REACH-AVOID	1.0	2	1	—
	5	0.95	REACH-AVOID REACH-STAY	0.4 0.6	[1, 2] 30	[1, 2] —	[0, 2] [0, 1]
	6	0.95	REACH-AVOID REACH-STAY	0.7 0.3	[1, 2] 60	[1, 2] —	[0, 2] [0, 1]
	7	—	REACH-AVOID REACH-STAY	0.8 0.2	[1, 2] 60	[1, 2] —	[0, 2] —
FALLOUTWORLD	1	0.95	REACH-AVOID	1.0	1	1	0.0
	2	0.9	REACH-AVOID	1.0	2	1	0.0
	3	0.9	REACH-AVOID	1.0	2	1	0.25
	4	0.9	REACH-AVOID	1.0	2	1	0.5
	5	0.9	REACH-AVOID	1.0	2	1	0.75
	6	0.9	REACH-AVOID REACH-STAY	0.8 0.2	[1, 2] 10	[1, 2] —	[0, 2] —
	7	—	REACH-AVOID REACH-STAY	0.95 0.05	[1, 2] 20	[1, 2] —	[0, 2] —

G.6. Implementation

Our implementation is built in JAX (Bradbury et al., 2018). We use Rabinizer 4 (Křetínský et al., 2018) to convert LTL specifications into LDBAs. All experiments were run on an NVIDIA GeForce RTX 5090 GPU.

H. Trajectory Visualizations

To verify that policies produced with PlatoLTL correctly satisfy the goal LTL specifications, we visualize example trajectories for *complex* LTL specifications in both *RGBZoneEnv* (Figure 6) and *FalloutWorld* (Figure 7), drawing from the continuous (i.e., infinite) sets of propositions.

I. Ablation Studies

I.1. Rate of Convergence over an Increasing Number of Training Propositions

We investigate how rate of convergence of PlatoLTL and the baselines vary as the number of training propositions is increased. Figure 8 presents evaluation curves for the *reach-avoid* LTL specifications in *RGBZoneEnv*, using training propositions drawn from a range of increasing $n \times n \times n$ RGB color grids spanning the full color space; the number of training propositions in each case is thus n^3 . These curves are summarized in Figure 9, which presents success rate and average episode length over an increasing number of training propositions, after 20M and 100M steps of training. We also include the evaluation curves for PlatoLTL on unseen propositions, drawn from $(n-1) \times (n-1) \times (n-1)$ grids interleaved within the training grids, except for the $2 \times 2 \times 2$ and $3 \times 3 \times 3$ training grids which both have a $4 \times 4 \times 4$ grid of unseen propositions interleaved within.

For the $2 \times 2 \times 2$ grid (8 propositions), we do not see a measurable benefit for PlatoLTL over the baselines on the training propositions. However, even here, the key strength of PlatoLTL is demonstrated in that its performance when evaluated on

unseen propositions remains comparable to that of the training set, despite a relatively small number of training propositions from which to generalize; the baselines are, by design, not capable of such generalization.

From the $3 \times 3 \times 3$ grid (27 propositions) onward, we see a clear divergence in performance during training between PlatoLTL and the baselines even on training propositions; the rate of convergence for the baselines decreases steadily as n is increased, while PlatoLTL is robust to this change and remains unaffected. This divergence is made clear in Figure 9a, and happens because the baseline approaches must learn a unique token embedding from scratch for each atomic proposition, and the number of embeddings to learn increases with the number of propositions. Meanwhile, PlatoLTL learns a single parameterized embedding for all propositions that are predicate instances of the same atomic predicate; adding more propositions simply provides more data for learning the mapping from predicate parameters to proposition embedding.

In summary, we see that rate of convergence for the baselines decreases steadily with the number of training propositions, to the point where required training time becomes impracticable, while (beyond a small threshold number of propositions) the rate of convergence does not decrease for PlatoLTL; thus, it remains feasible to apply PlatoLTL as the number of propositions becomes very large (or even infinite), so long as those propositions can be represented as predicate instances of the same set of atomic predicates.

I.2. Evaluation Performance at Convergence When the Number of Training Propositions is Large

We investigate how evaluation performance (success rate and average episode length) of PlatoLTL and the baselines compare when the number of training propositions is large. We consider *reach-avoid* LTL specifications in *RGBZoneEnv* using the $11 \times 11 \times 11$ grid, as in Section 7, but we now train for 500M environment interactions rather than 100M. Figure 10 presents the training and evaluation curves.

While the baselines have still not converged after 500M interactions (meanwhile, PlatoLTL has converged well within 100M interactions), we can see from Figure 10a that they have at least reached the final curriculum stage, and we can see from Figure 10b that their success rates and average episode lengths on training propositions are converging asymptotically towards that of PlatoLTL.

This confirms our observations from the results for *FalloutWorld* in Section 7 (wherein the baselines were close to convergence); upon convergence, the baseline methods offer similar evaluation performance to PlatoLTL on training propositions. However, when the number of training propositions is large, convergence for the baselines may require an impractically long training time (see Appendix I.1), thus PlatoLTL produces superior performance given a reasonable training time.

I.3. Evaluation Performance of Baseline Methods on Unseen Propositions

We emphasize that PlatoLTL’s key strength is its ability to generalize to unseen propositions through parameterization, which existing methods in multi-task LTL-guided RL do not have the capability to exploit. To demonstrate this, we consider again the experiment in Appendix I.2, and employ a naïve solution for the baselines wherein a new embedding is initialized for each unseen proposition (or assignment, in the case of DeepLTL). Figure 10b presents evaluation curves for the set of unseen propositions; while the performance of PlatoLTL remains at parity with that for training propositions, we see that the baselines fail to generalize under the naïve solution, with very low success rate and very high average episode length (as we would expect). Note that we would see a similar trend for *FalloutWorld*.

I.4. Principal Component Analysis of Proposition Embeddings

This ablation study tests our claim that PlatoLTL achieves generalization by learning a shared structure across related propositions in embedding space, and that existing methods cannot generalize since they do not exploit this structure. We perform a principal component analysis (PCA) of the learned proposition embeddings for policies produced using PlatoLTL and the baseline methods, considering both the training propositions and unseen evaluation propositions as described in Appendix G.5.

Figures 11 and 12 present the results. Qualitatively, we see that for *RGBZoneEnv*, the PCA for PlatoLTL produces a (slightly deformed) cube for the *at* predicate, encapsulating the RGB color space of the colored zones, with excellent interpolation of unseen proposition embeddings. For *FalloutWorld*, the PCA for PlatoLTL produces a (deformed yet smooth) plane for the *loc* predicate, encapsulating the grid of possible coordinates, and a line (at some distance away from the plane) for the *rad*

predicate, representing the range of possible radiation intensity thresholds. Meanwhile, for the baselines we see no inherent relationship between the embeddings of the propositions, and the PCA looks like noise for both environments.

Quantitatively, we see that PlatoLTL achieves 95.7% total explained variance between the 3 principal components in *RGBZoneEnv*, and 89.2% in *FalloutWorld*. These high values mean that PlatoLTL has learned a low-dimensional representation, where the embedding space is organized almost entirely along a 3D manifold. Since the predicate parameters themselves are low-dimensional (3D at most), this suggests a smooth, continuous mapping wherein the structure of the propositions is well-preserved in the embedding space, thus enabling generalization.

Meanwhile, the baselines achieve 11.2% total explained variance between the 3 principal components in *RGBZoneEnv*, and 13.7% in *FalloutWorld*. These very low values mean the embeddings are high-dimensional and scattered, and the principal 3 components barely capture any pattern. This also tells us that a naïve attempt at parameterization by linearly interpolating between proposition embeddings according to their parameters would fail.

In summary, we observe that PlatoLTL learns the underlying structure relating the propositions, thus facilitating generalization, whereas the baselines essentially memorize a dictionary of independent embeddings. Furthermore, PlatoLTL learns individual geometries for each predicate (e.g., the plane for the *loc* predicate and the line for the *rad* predicate in *FalloutWorld*), placing these distinct shapes in separate parts of the embedding space.

I.5. Number of Training Propositions Required for Generalization

Through the results of Section 7, we have established that, given a sufficiently large set of training propositions, PlatoLTL generalizes to unseen propositions at evaluation time. This ablation study investigates the natural follow-up question: how many training propositions are required to achieve good generalization? Or, more formally, how does evaluation performance on unseen propositions vary with the size of the set of training propositions? Ideally, we would like to achieve generalization given a small (yet representative) training set.

For both environments, we train the agent using different numbers of fixed training propositions sampled randomly from the full set of possible propositions, and evaluate on *reach-avoid* LTL specifications composed from propositions drawn from the full set. For *RGBZoneEnv*, we train the agent using a fixed set of colors sampled randomly from the RGB color space, then evaluate on colors drawn from the continuous color spectrum. To obtain a training set that is representative of the color space, we iteratively apply farthest-point sampling (with some noise) to sample each color after the first (which is sampled uniformly from the color space). For *FalloutWorld*, we train the agent using a fixed set of locations sampled uniformly from the grid, then evaluate on locations drawn from the full grid. For simplicity, we sample from the continuous range of radiation thresholds during both training and evaluation; the number of training propositions thus refers specifically to the number of training propositions for location.

The results are presented in Figure 13. For both environments, we observe that increasing the number of training propositions increases the success rate and decreases the average episode length, approaching the results of Figure 3. For *RGBZoneEnv*, we see that training on the minimum of 4 training propositions results in a 70% success rate on *reach-avoid* specifications, which rises to 95% by only 6 propositions, and converges to 98% by as few as 8 propositions. This is an incredibly low number of training propositions for generalization, given that we evaluate on the full RGB color space, drawing from an infinite number of unseen propositions. Meanwhile, *FalloutWorld* requires a considerably larger number of training propositions for generalization; while evaluation performance is poor for 32 training propositions, we see a sharp rise surpassing 80% success rate by 64 propositions, and convergence to 93% success rate by 160 propositions (which cover 36.3% of the total grid).

We thus observe that the number of training propositions required for generalization depends strongly on the nature of the environment and the propositions themselves, though for both environments studied in this paper, this number is relatively low.

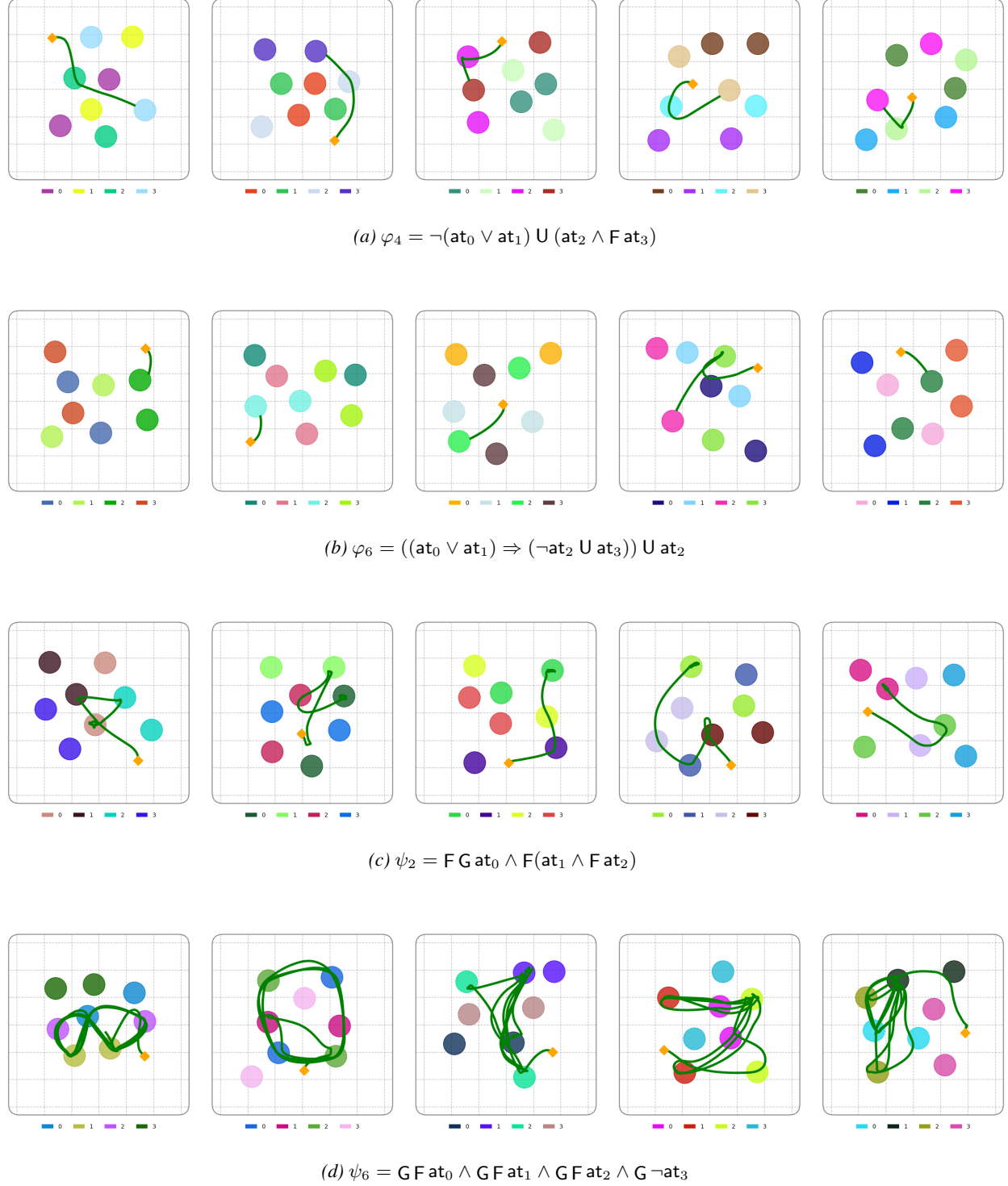


Figure 6. Example trajectories of PlatoLTL for complex LTL specifications in *RGBZoneEnv*, drawing from an continuous (i.e., infinite) set of propositions. All trajectories were generated using the same trained policy. Note that all trajectories shown satisfy the specifications.



Figure 7. Example trajectories of PlatoLTL for complex LTL specifications in *FalloutWorld*, drawing from an continuous (i.e., infinite) set of propositions. All trajectories were generated using the same trained policy. The locations loc_0 , loc_1 and loc_2 have been annotated with “A”, “B” and “C” respectively, and grid tiles with shaded lines illustrate where the rad_0 proposition is true. Note that all trajectories shown satisfy the specifications.

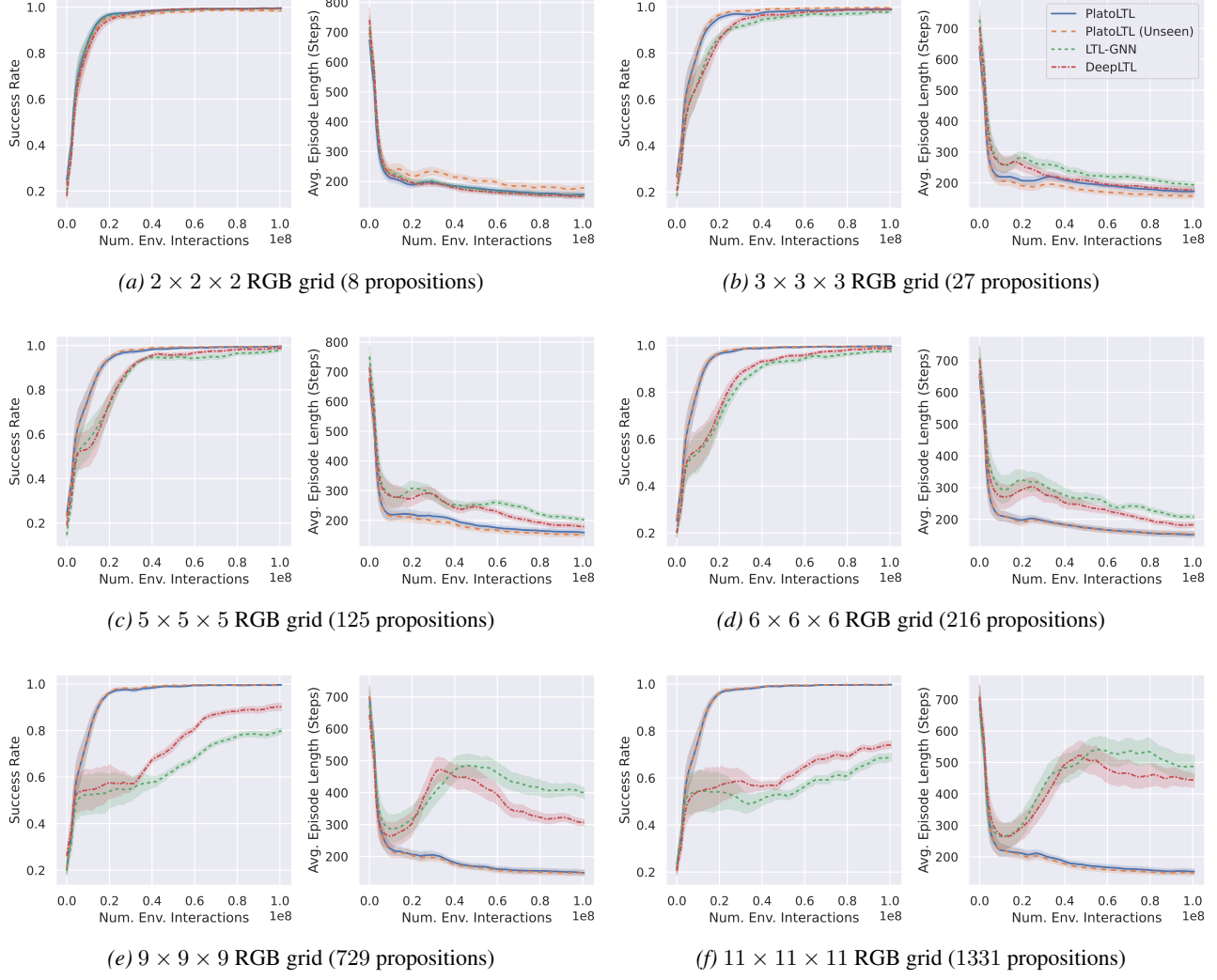


Figure 8. Success rate (as a proportion of total roll-outs) and average episode length (in steps) during training for *reach-avoid* LTL specifications in *RGBZoneEnv*, using training propositions drawn from a range of increasing $n \times n \times n$ RGB color grids spanning the full color space. Results are averaged over 5 seeds, 50 specifications per seed and 16 episodes per specification per seed, with 95% confidence intervals marked by the shaded area.

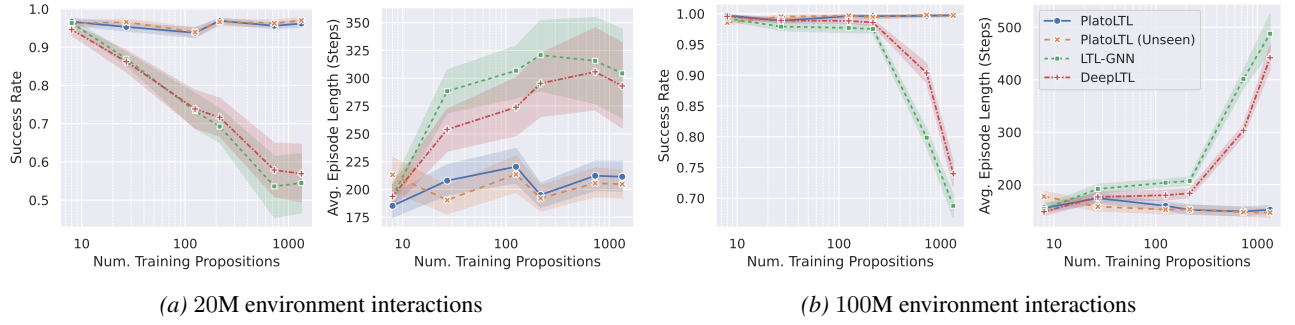
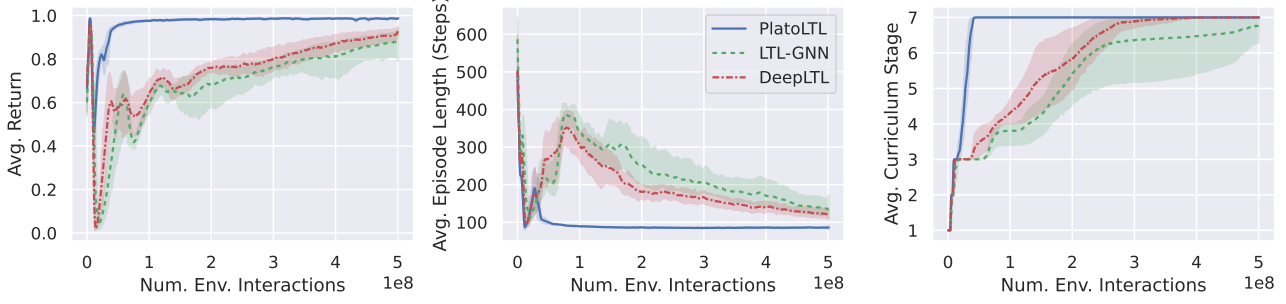
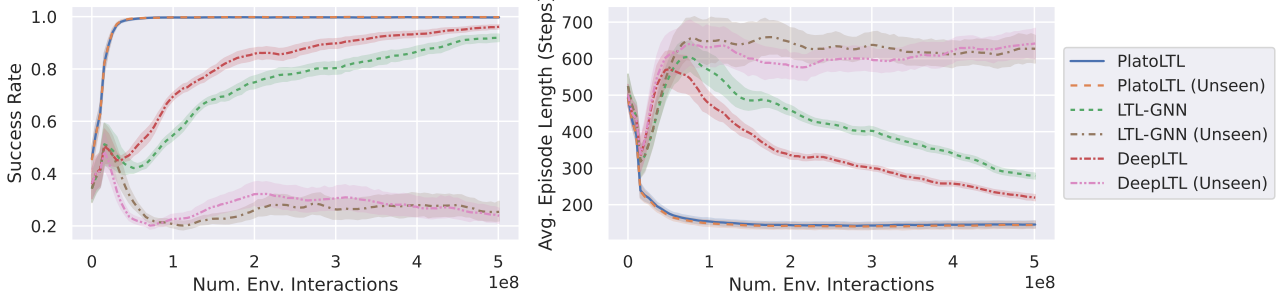


Figure 9. Success rate (as a proportion of total roll-outs) and average episode length (in steps) after a number of total environment interactions during training for *reach-avoid* LTL specifications in *RGBZoneEnv*, using training propositions drawn from a range of increasing $n \times n \times n$ RGB color grids spanning the full color space. Results are averaged over 5 seeds, 50 specifications per seed and 16 episodes per specification per seed, with 95% confidence intervals marked by the shaded area.



(a) Average return, episode length (in steps) and curriculum stage during training. Results are averaged over 5 seeds, with 95% confidence intervals marked by the shaded area. Note the initial spike in average return; this is due to the first two curriculum stages not including any “avoid” propositions, meaning the agent could achieve high return by simply driving between zones without any sense of color understanding. Thus, average return plummets sharply once “avoid” propositions are introduced in the third stage; note PlatoLTL recovers much faster than the baselines.



(b) Success rate (as a proportion of total roll-outs) and average episode length (in steps) during training for *reach-avoid* LTL specifications, composed from the training set of atomic propositions. Results are averaged over 5 seeds, 50 specifications per seed and 16 episodes per specification per seed, with 95% confidence intervals marked by the shaded area.

Figure 10. Training and evaluation curves for *RGBZoneEnv* over 500M environment interactions.

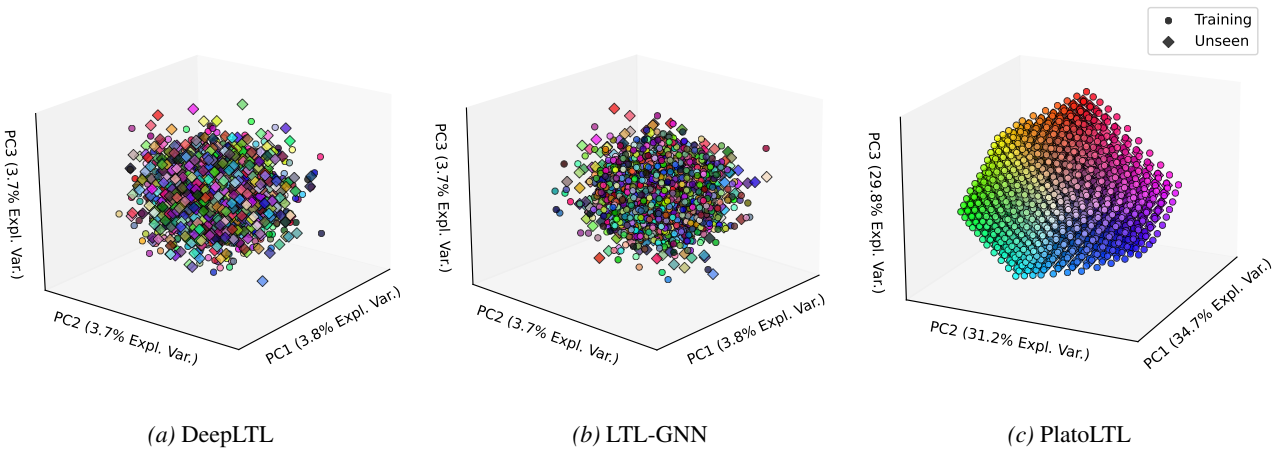


Figure 11. Principal component analyses of learned proposition embeddings for policies produced with each method in *RGBZoneEnv*. Circles are training propositions, diamonds are unseen (evaluation) propositions. The data point for a predicate instance $\text{at}(r, g, b)$ has the RGB value (r, g, b) . The explained variance of each principal component is also listed.

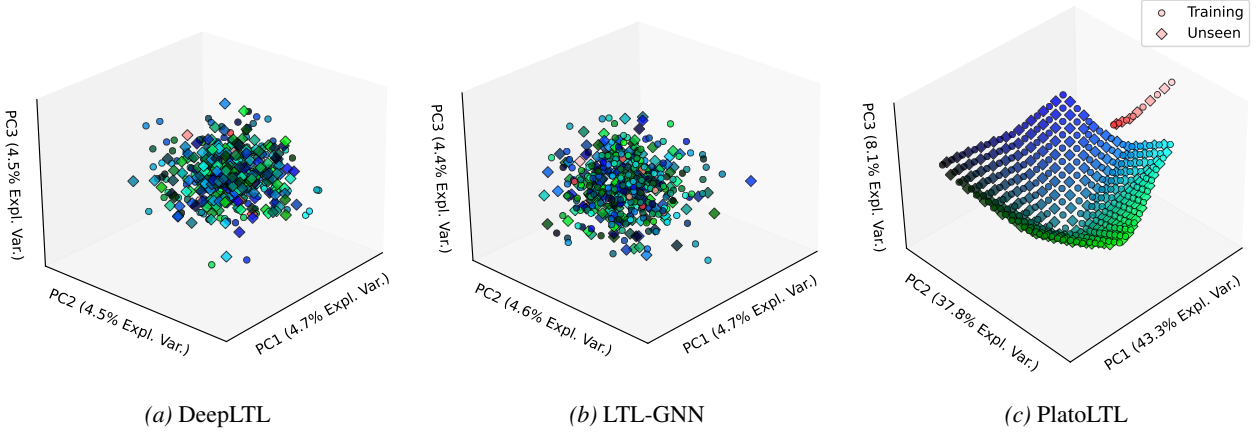


Figure 12. Principal component analyses of learned proposition embeddings for policies produced with each method in *FalloutWorld*. Circles are training propositions, diamonds are unseen (evaluation) propositions. The data point for a predicate instance $\text{rad}(tol)$ has the RGB value $(1, 1 - tol, 1 - tol)$ such that color transitions from white to red as radiation intensity threshold increases, and the data point for a predicate instance $\text{loc}(x, y)$ has the RGB value $(0, x, y)$, where x and y are normalized to $[0, 1]$, such that increasing the x -coordinate increases greenness and increasing the y -coordinate increases blueness. The explained variance of each principal component is also listed.

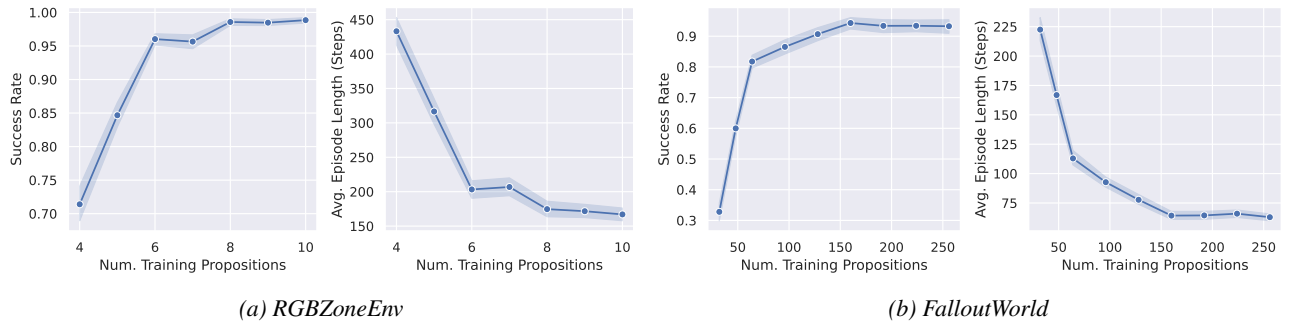


Figure 13. Success rate (as a proportion of total roll-outs) and average episode length (in steps) for PlatoLTL for *reach-avoid* LTL specifications, using different numbers of fixed training propositions and evaluating on the full set of possible propositions. Results are averaged over 5 seeds, 50 specifications per seed and 16 episodes per specification per seed, with 95% confidence intervals marked by the shaded area.